Function and evolution of the atypical Notch ligands *Dlk1* and *Dlk2* during vertebrate development

Benjamin Shaw

University of Cambridge
Department of Physiology, Development and Neuroscience
Peterhouse College

April 2017

This dissertation is submitted for the degree of Doctor of Philosophy

Declaration

I hereby declare that my thesis entitled 'Function and evolution of the atypical Notch ligands Dlk1 and Dlk2 during vertebrate development' is a result of my own work and includes nothing which is the outcome of work done in collaboration or which has been submitted for a previous degree except when specifically indicated in the text.

Benjamin Shaw

Statement of Length

This dissertation does not exceed the word limit for the Degree Committee for the Faculty of Biology.

Benjamin Shaw

PhD abstract

Delta-like homologue 1 (*Dlk1*) and *Dlk2* encode vertebrate-specific transmembrane proteins belonging to the *Jagged/Delta/Serrate* family of Notch ligands. Murine *Dlk1* is widely expressed during embryonic development and targeted deletion results in defects in numerous developmental processes, such as adipogenesis, haematopoiesis, neurogenesis and skeletal muscle formation. However, the mechanisms by which DLK1 regulates these processes remains unclear. The purpose of this project is to examine the function of these genes using zebrafish as an *in vivo* model, allowing insight to the ancestral functions of these genes. We have strong evolutionary evidence that *dlk2* is the ancestral version of the gene from which *dlk1* is derived; therefore, the thesis focuses primarily on the role of *dlk2* in the zebrafish system.

I initially examine the expression of zebrafish *dlk1* and *dlk2* during embryonic development and in the adult brain, determining similarities and differences between mouse and zebrafish. In particular, *dlk1* and *dlk2* in the fish exhibit a pattern that is more reminiscent of *Dlk2* in the mouse. This developmental expression pattern is essential for the interpretation of the modulation of Dlk2 in later chapters, and is aided by the generation of a mammalian Dlk2 antibody that cross-reacts with zebrafish. We obtained a *dlk2* mutant and used this line to examine the role of the DLK2 protein in development and in the adult brain. I demonstrate that, in the absence of DLK2, a population of neural precursor cells appear to over-proliferate early in zebrafish development. Later, by larval stages, these cells are absent, suggesting a premature activation and subsequent depletion of the progenitor cell pool in the mutant, reminiscent of the *Dlk1* mutant in mouse. Associated with this phenotype are larval behavioral defects in motor response. In this thesis, it will be shown that in the adult *dlk2* mutant zebrafish, the radial glial cell population in the telencephalon is completely depleted. These radial glial cells are thought to be responsible for adult neural regeneration in zebrafish, and our characterization of a mutant completely lacking this cell population provides a rich model to further examine and understand the functions of this well-

studied but poorly understood cell population. These findings have both functional and evolutionary implications for the relative roles of these two vertebrate specific atypical Notch ligands.

Acknowledgements

Firstly, I would like to thank the Wellcome Trust for funding my PhD, making it possible for me to pursue this project. I would also like to thank the Developmental Biology PhD Programme at the University of Cambridge, and in particular Clare Baker. I would like to thank all of the fish room staff, their hard work made all of these experiments possible. I am very grateful to Anne Wiblin for collaborating with us to produce a Dlk2 antibody, which has played a big role in this project. Bill Budenburg from Zanticks very graciously donated a tracking rig to the lab and has been providing support for an ongoing collaboration, and I am very grateful for his help.

I am extremely grateful of Anne Ferguson-Smith for her supervision throughout this project and all her support, both in the lab and personally. Everyone in the Ferguson-Smith lab has been a joy to be around and has really made the experience worthwhile. Angie Fleming has been an incredible support to me throughout the PhD, but particularly in the really difficult times when she was there to save the day. During the writing up process, she worked so hard to help me and I will be eternally grateful for that. I'm very grateful to everyone in Angie's lab for putting up with me everyday, putting up with my mess and constant noise. Thank you to them in particular for making me laugh everyday, no matter how hard the day. Aileen Briggs has been a huge support to me during this PhD, and without her support I am certain I would not have submitted this report.

I really value the friendships I have made during the PhD, I'm sure they will stay with me for life. I am particularly grateful to have met my fiancée, Sonia Nestorowa, while in the lab. Many difficult events have happened over the last few years but she has been a rock of support and she is responsible for anything I have achieved. Gustavo Cerda-Moya became a close friend late on in my PhD, but he has been a huge support to drive me to finish it and I would like to thank him for that. Lastly, I would like to thank Sophie Miller. She was a great friend to me throughout my PhD, a great teacher of various *in situ* protocols, and it was a blessing when she got a post-doc to look

at *dlk1* in zebrafish liver regeneration. I would like to thank her supervisor, Elke Ober, for allowing us to collaborate on this project. It was an incredible injustice that she was taken well before her time, and she is sorely missed.

Table of contents

List of figures

List of Abbreviations

Abbreviation	Full Name
AGM	Aorta-gonad-mesonephros
ANOVA	Analysis of Variance
BAT	Brown adipose tissue
BrdU	Bromodeoxyuridine
BSA	Bovine Serum Albumin
cDNA	Complementary Deoxyribonucleic Acid
cKO	Conditional Knockout
CRISPR	Clustered regularly interspaced short palindromic repeats
DAPI	4'-6-diamidino-2-phenylindole
d.p.f.	days post fertilization
dH2O	Distilled Water
DLK1	Delta-like homologue 1
DLK2	Delta-like homologue 2
DLL	Delta-like
DMSO	Dimethyl Sulfoxide
DNA	Deoxyribonucleic Acid
DNAse	Deoxyribonuclease
DOS	Delta and OSM-11
DSL	Delta-Serrate-Lag2
E	Embryonic day (of mouse development)
E3M	Embryo Medium
EDTA	Ethylenediamine Tetraacetic Acid
EGF	Epidermal Growth Factor
ERK	extracellular signal–regulated kinases
ESC	Embryonic stem cell
g	Gram
GFAP	Glial Fibrillary Acidic Protein
GFP	Green Fluorescent Protein
h.p.f.	hours post fertilization
HEPES	4-(2-hydroxyethyl)-1-piperazineethanesulfonic acid
HSC	hematopoietic stem cell
HuC	embryonic lethal, abnormal vision, Drosophila-like 3
Hz	Hertz
IG-DMR	Intergenic differentially methylated region
IHC	Immunohistochemistry
ISH	*In situ* hybridization
KO	Knockout
Mg	Microgram
µL	Microlitre
MAP	Mitogen-activated protein
MEF	Mouse Embryo Fibroblast
MEK	mitogen-activated protein kinase kinase
Mg	Milligrams
mL	Millilitres

mESC	Mouse Embryonic Stem Cell
MM	Mismatch
MO	Morpholino Oligonucleotide
MOVEM	
mRFP	Monomeric Red Fluorescent Protein
mRNA	Messenger Ribonucleic Acid
ng	Nanograms
NICD	Notch intracellular domain
nL	Nanolitre
NSC	Neural stem cell
NST	Non-shivering thermogenesis
p53	protein 53
PAGE	Polyacrylamide Gel Electrophoresis
PBS	Phosphate Buffered Saline
PCNA	Proliferating cell nuclear antigen
PCR	Polymerase Chain Reaction
PFA	Paraformaldehyde
prim	Primordium
PTU	1-phenyl 2-thiourea
RBP-jk	J kappa-recombination signal-binding protein
RNA	Ribonucleic Acid
RNAse	Ribonuclease
rtPCR	Reverse Transcriptase Polymerase Chain Reaction
SDS	Sodium Dodecyl Sulfate
SVZ	subventricular zone
TALEN	Transcription activator-like effector nucleases
TBE	Tris/Borate/EDTA
Tricaine	Ethyl 3-aminobenzoate methanesulfonic acid
TUNEL	Terminal deoxynucleotidyl transferase dUTP Nick End Labeling
UV	Ultraviolet

1. Introduction

1. Introduction

The gene *Dlk1* is known to have numerous functions during mouse development. While this gene has been extensively studied and has been shown to regulate many processes, the mechanisms via which it functions are largely unknown and have so far been difficult to elucidate and confirm using the mouse model. Murine *Dlk1* has a juxtamembrane cleavage site that allows it to be secreted. Alternative splicing of *Dlk1* leads to this site being either included or excluded from the mature transcript, hence resulting in different transcripts that are either secreted or membrane-bound. The different isoforms of the DLK1 protein have different functions during development, which makes understanding their function and mechanisms of function *in vivo* very challenging. Murine *Dlk1* has also been co-opted into numerous mammalian specific functions, and is regulated as part of an imprinted cluster, potentially making it easier to understand basal mechanisms of function in a non-mammalian system. A similar gene, *Dlk2*, has also been described. It is structurally very similar to *Dlk1*, but currently very little is known about its function. However, evolutionary analysis suggests that *Dlk2* is the ancestral gene from which *Dlk1* is derived. This project aims to examine *dlk1* and *dlk2* in zebrafish to establish a model system in which it will be possible to elucidate the currently unknown mechanisms by which these genes operate.

This chapter presents an overview of what is currently known about these genes, starting with their structure and evolution. Current knowledge about the expression of *Dlk1* in mouse will be explained as well as compared to *dlk1* expression in zebrafish, in both development and post-natal life. Particular attention will be paid to the known functions of *Dlk1* and its role in stem cell regulation. It is hypothesized that the regulation of stem cells may represent the conserved and ancestral functions of these genes, as opposed to the highly mammalian functions *Dlk1* performs in mouse. Therefore, these examples provide a useful context in which to examine the possible roles these genes play in zebrafish, and to interpret the results presented in this thesis. The known neo-functionalism observed in the murine system is examined in order to provide further

understanding of these genes, but also to demonstrate the difficulty of examining these genes within the murine system. The zebrafish system is introduced as an ideal model to examine the function of these genes. The chapter is concluded with a summary of the hypotheses addressed in this thesis.

1.1 The protein structures of murine DLK1 and DLK2

Delta-like homologue 1 (*Dlk1*) encodes a vertebrate-specific transmembrane protein which belongs to the *Jagged/Delta/Serrate* family of Notch ligands (Bray et al., 2008; Ferrón et al., 2011). Proteins in this family typically contain a series of Epidermal Growth Factor (EGF)-like repeats and a *Delta-Serrate-Lag2* (DSL) domain at the N terminus. The DSL domain is thought to be the domain which interacts with the EGF-like repeats of Notch proteins (Cordle et al., 2008). *Dlk1* contains six of these tandemly repeated EGF-like motifs; however, these lack the conserved residues thought to be required for binding to EGF receptors (Laborda et al., 1993; Sul, 2009). Instead, the two most N-terminal EGF-like repeats of the DLK1 protein are a conserved DOS (*Delta and OSM-11*) motif, shared by the classic Notch ligands (Kopan and Ilagan, 2009). *Dlk1* significantly differs from the other members of this family in two main aspects: it has a short intracellular domain and no DSL domain (Bray et al., 2008) (Fig. 1.1A). In *Drosophila*, Delta proteins with similarly truncated intracellular domains act as dominant-negative forms of Notch ligands (Sun and Artavanis-Tsakonas, 1996). DLK1 contains a juxtamembrane motif that can be cleaved by extracellular proteases. In eutherian mammals, alternative splicing creates different transcripts encoding four different protein isoforms (Fig. 1B). There are two secreted isoforms that contain the motif (A and B), and two that do not contain the protein cleavage site and as such remain membrane-bound (C and D) (Bray et al., 2008). These isoforms have been shown to play different developmental roles (Baisong Mei, 2002; Ferrón et al., 2011).

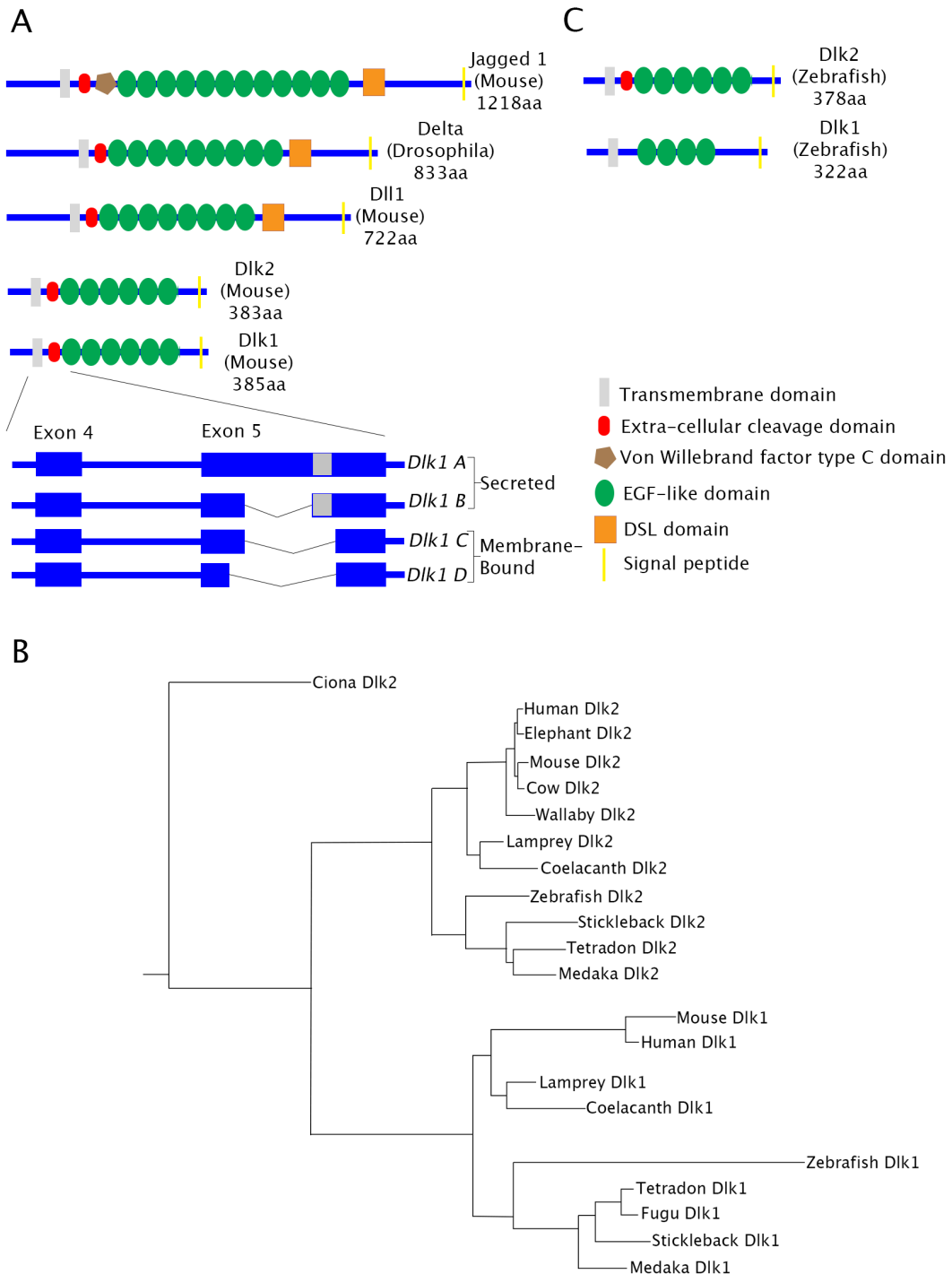

Figure 1.1 | Structure and evolution of DLK1 and DLK2. A Diagrams of the major structural components of classic Notch ligands in comparison to DLK1 and DLK2. An illustration of the alternatively spliced isoforms of murine *Dlk1*. Adpated from (Bray et al., 2008; Ferrón et al., 2011). B Maximum likelihood tree of *Dlk1* and *Dlk2* evolution produced using PhyML (Carol Edwards). C Diagram of the major structural components of zebrafish DLK1 and DLK2.

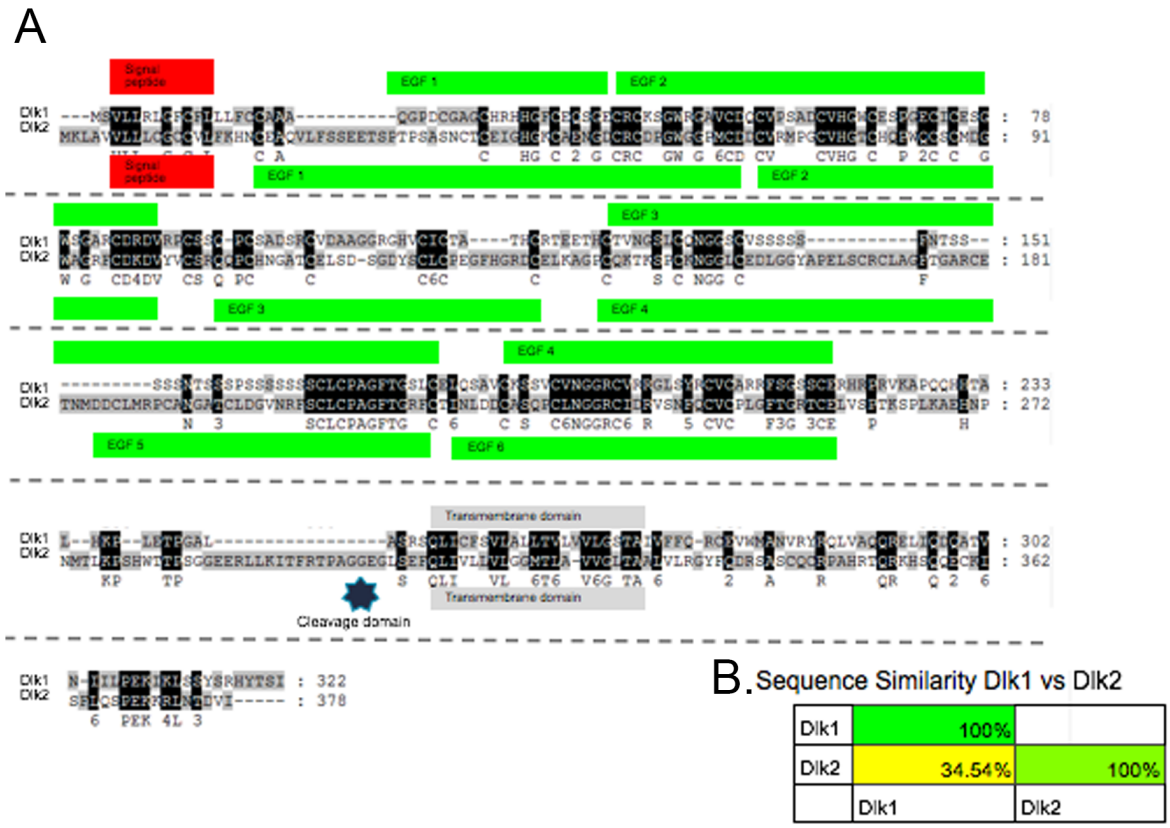

Figure 1.2 | Comparative protein structure of zebrafish Dlk1 and Dlk2. A The protein between zebrafish Dlk1 and Dlk2 (aligment performed with GeneDoc software). The protein domains have been manually labelled. **B.** A sequence similarity was performed using the SIM online alignment tool.

1.2 Evolution of of DLK1 and DLK2 in vertebrates

1.2.1 *Dlk2* is the ancestral gene and highly conserved among the vertebrate species

Delta-like originally arose from the duplication of Delta at some point before the divergence of *Ciona* from the rest of the chordate lineages (Fig. 1.1B, pers. comm. Carol Edwards). A subsequent duplication produced *Dlk1* and *Dlk2*. *Dlk2* is much more highly conserved than *Dlk1* in all species examined. In *Ciona*, where there is only one *Dlk* gene, it is more similar to mammalian *Dlk2* than to *Dlk1,* suggesting that this is the ancestral form.

1.2.2 Zebrafish *dlk1* lacks the sequence for the cleavage domain.

Zebrafish have a single copy of both *dlk1* and *dlk2*, but zebrafish *dlk1* is highly divergent to *Dlk1* examined in all other species (Fig 1.1B). Zebrafish *dlk1* lacks the sequence for the extracellular cleavage site and so remains tethered to the membrane. *Dlk2,* on the other hand, still contains the cleavage site (Fig.1.1C). Comparing their protein structure demonstrates the similarity between these proteins and also clearly shows the loss of the juxtamembrane cleavage site (Fig. 1.2).

1.3 Murine *Dlk1*

1.3.1 *Dlk1* expression during embryonic development

Dlk1 has been examined at E10, E12.5 and E16.5 and is clearly widely expressed during early embryonic development. The period between E12.5 and E16.5 marks the period of reduced *Dlk1* expression. In postnatal mice, it is isolated to a few specific tissues; in the brain, this includes the

nucleus accumbens, the sub-ventricular zone and several areas of the hypothalamus (da Rocha et al., 2007; Yevtodiyenko and Schmidt, 2006).

Between E10 and E16.5, *Dlk1* is expressed in tissues derived from the ectodermal, mesodermal, endodermal cells layers, as well as extra-embryonic tissues. In ectodermally-derived tissues, *Dlk1* is isolated to a few specific locations, such as the thalamus, hypothalamus and the optic recess (da Rocha et al., 2007). *Dlk1* is prominently expressed in the Rathke's pouch from E10 to E13, which then forms the anterior lobe of the developing pituitary gland. At E15, *Dlk1* is expressed in the mature pituitary gland in the anterior lobe but also more strongly expressed in the independently-derived posterior lobe. In contrast to its expression in the ectoderm, *Dlk1* is more broadly expressed in the mesoderm during murine embryonic development. At E10, *Dlk1* is expressed in the myotomes and the sclerotome of the somites, and is expressed in skeletal muscle and cartilage until birth (da Rocha et al., 2007). The tongue is one of the most highly *Dlk1* expressing tissues at E12.5 and this expression is maintained, as with the other skeletal muscle expression, through E16.5 until birth (Yevtodiyenko and Schmidt, 2006). *Dlk1* is expressed in most undifferentiated mesenchyme at this early stage (Yevtodiyenko and Schmidt, 2006). In endodermally-derived tissues, *Dlk1* is most strongly expressed in the lung and in the liver. In the developing liver, *Dlk1* is highly expressed in the hepatic cells. In the lung, *Dlk1* is expressed in the segmental bronchi and surrounding mesenchyme at E12.5. By E16.5, there is a reduction of *Dlk1* expression in the lung but it remains in the epithelium of the terminal bronchioles (Yevtodiyenko and Schmidt, 2006). *Dlk1* is also expressed in the pancreas and the ducts of the adrenal gland (da Rocha et al., 2007). *Dlk1* is expressed throughout extraembryonic tissues, including the chorionic plate, yolk sac and placenta (da Rocha et al., 2007). *Dlk1* is also expressed in all three layers of the placenta: the labyrinthine zone, junctional zone and decidua basalis (da Rocha et al., 2007)

Dlk1 is most likely expressed in more locations than has currently been described in these gross morphological studies. As will be described in Section 1.4, *Dlk1* is also expressed in numerous stem cell and progenitor cell populations, playing a key role in the differentiation and

proliferative states of these cells. These discrete cell populations mostly likely account for the majority of *Dlk1* expression in the postnatal and adult mouse.

1.3.2 Development of the *Dlk1* mutant mouse

Given the expression of *Dlk1* throughout all the different germ-layer derived tissues, and its key roles in stem cell regulation (Section 1.4), it is worth noting that *Dlk1*-null mice are homozygous viable from zygotic mutants. The *Dlk1* mutant mice were found to be growth retarded, with female mutant mice weighing an average of 7.34g and males weighing 7.58g, compared to the wild type averages of 8.51g and 8.81g, respectively (Moon et al., 2002). In addition, when fed on a high-fat diet, the level of adipose deposition in white fat pads was increased in mutant mice relative to the wild type in both males and females. By examining differentiation markers in the adipose tissue, it was determined that increased levels of pre-adipocyte differentiation were responsible for the increased level of fat pad weights (Moon et al., 2002). This is in line with the proposed role of *Dlk1* in adipogenesis (Section 1.4.1). Overall, the gross morphological effects of losing *Dlk1* are not as dramatic as might be expected. The *Dlk1*-null mouse has been used to examine specific roles of *Dlk1* in different cell populations and to study *Dlk1* as a stem cell regulator, described in Section 1.4.

1.4 *Dlk1* as a stem cell regulator

1.4.1 *Dlk1* in adipogenesis

During adipogenesis, *Dlk1* is highly expressed in pre-adipocytes and is then down-regulated during differentiation into adipocytes, being completely absent in the mature adipocyte. *In vitro,* the presence of *Dlk1* inhibits differentiation of pre-adipocytes into adipocytes (Smas and Sul, 1993). To demonstrate this, *Dlk1* was expressed in 3T3-L1 cells, a pre-adipocyte cell line, using a constitutively active expression plasmid with *Dlk1* cDNA. The markers of mature adipocytes were examined, showing a reduction in adipogenesis in the *Dlk1* expressing cells *in vitro* compared to the empty control vector (Wang et al., 2006). The same system was used to explore the effect of only expressing one of each of the four isoforms (outlined in section 1.1). The result of the isoforms is a protein that is either tethered to the membrane or able to be secreted because of the inclusion of the extra-cellular cleavage site. This experiment demonstrated that only the isoforms able to produce the large soluble form of *Dlk1* (DLK1A and DLKB) display the inhibitory role on adipogenesis. The isoforms that are membrane-tethered had no effect on the differentiation of 3T3-L1 cells into mature adipocytes *in vitro* (Wang et al., 2006). This demonstrates that the secreted isoform and the membrane-bound isoform perform distinct developmental roles. As predicted from the *in vitro* results, the *Dlk1* mutant mice have increased levels of obesity (Moon et al., 2002). This is assumed to be as a result of losing the secreted DLK1 protein, but as both are expressed from the same deleted gene locus, it is impossible to definitively identify which isoform is responsible.

1.4.2 *Dlk1* in haematopoietic stem cells

Dlk1 is known to be expressed in the major sites of haematopoiesis in the developing embryo, such as the placenta and the liver (See section 1.3.1). In order to examine the possible role of *Dlk1* in haematopoiesis, the number of hematopoietic stem cells (HSCs) was examined *in vivo* in the wild type, the *dlk1* mutant and in a transgenic mouse that expresses an extra copy of *dlk1* from a different genetic locus but under the control of the endogenous *dlk1* promoter (Mirshekar-Syahkal et al., 2013). The aorta-gonad-mesonephros (AGM) is an important site of HSC production during definitive haematopoiesis, starting at E10 (Dieterlen-Lievre, 1975). The AGM was examined at E11.5, and absence of *Dlk1* led to an increase in the number of haematopoietic stem and progenitor cells present, with a similar decrease observed in the transgenic *Dlk1* over-expressing embryo. Tunnel assays and Ki67 staining were performed to investigate apoptosis and differentiation, respectively, and demonstrated that, in the *Dlk1* mutant, there were increased levels of the differentiation marker and the differences in cell populations between the conditions were not because of apoptosis levels. The number of HSCs in the mutant or transgenic AGM was not altered (Mirshekar-Syahkal et al., 2013). Taken together, this demonstrates that *Dlk1* is negatively regulating the differentiation of HSCs, as it does with pre-adipocytes.

1.4.3 *Dlk1* in neural progenitor development

The role *Dlk1* plays in mammalian embryonic neurogenesis was assessed using an *in vitro* model. Embryonic stem cells (ESCs) were differentiated into neural progenitor cells (Surmacz et al., 2011). In the wild-type, *Dlk1* expression corresponded with the expression of the pro-neural genes *Mash1* and *NeuroD*. To examine the role of *Dlk1*, a tamoxifen-induced *Dlk1* expression construct was used to up-regulate *Dlk1* levels in the differentiating cell population. In this context, the up-regulation of *Dlk1* led to an increase in neural differentiation, using p57Kip2 as a differentiation marker (Surmacz et al., 2011). This same effect was observed if the medium from the *Dlk1* over-

expressing cells was used to culture wild-type ESC-derived neural progenitor cells, suggesting this process is mediated by the secreted isoform of *Dlk1*.

1.4.4 *Dlk1* in adult neurogenesis

Neural stem cells (NSCs) are not only present in the embryonic mouse, but also in isolated areas of the adult brain. In particular, NSCs have been found in the subventricular zone (SVZ) and the hippocampus (Ma et al., 2009). A recent study found that while mouse *Dlk1* is dispensable for neurogenesis, it is important for maintaining NSC populations in the neurogenic niche of the SVZ (Ferrón et al., 2011). As the *Dlk1*-null mutant animals age, the amount of primary neuroblasts decrease because the NSC pool is not properly maintained. NSCs were isolated from the post-natal mouse, and it was shown that applying recombinant DLK1 to the medium led to an increased number of neurospheres being produced from these wild type NSC cultures. The neurosphere assay is an established technique to assess NSCs, and the neurospheres are a heterogeneous population of NSC progeny (Reynolds and Rietze, 2005) However, neurosphere production by NSCs derived from the *Dlk1*-null mouse did not increase with the addition of recombinant DLK1 (Ferrón et al., 2011). By specifically expressing the membrane-bound *Dlk1* or the secreted *Dlk1* in the *Dlk1*-null NSCs, it was demonstrated that the NSCs need to express the membrane-bound form of DLK1 in order for the recombinant DLK1 in the media to cause an increase in the neurosphere production. In the SVZ, the NSCs are surrounded by niche astrocytes, and it was hypothesized that these could be the *in vivo* source of the secreted DLK1. Co-culture experiments with NSC and *dlk1*-null niche astrocytes transfected with the different isoforms of *Dlk1* demonstrated that the expression of the secreted form of DLK1 from the niche astrocytes increased the neurosphere production in wild type NSCs (Ferrón et al., 2011).

In summary, the niche astrocytes normally regulate NSC proliferation and differentiation into neuroblasts by expressing the secreted form of *Dlk1*. However, this signal can only be received

by NSCs if they are expressing the membrane-bound form of *Dlk1* (Ferrón et al., 2011) This raises a series of questions regarding the relationship between the membrane-bound and secreted isoforms, receptor-ligand interactions, and the signaling pathways of the different isoforms. Deciphering these questions *in vivo* in mouse is difficult, because it is challenging to modulate the different isoforms separately as they are expressed from the same gene locus.

1.5 *Dlk1* mammalian neofunctionalism

1.5.1. *Dlk1* has roles in mammalian-specific functions

One of the largest challenges a mammal faces is the transition to independent life. One of the key process involved with this transition is the shift in their metabolic mode from lipolytic to lipogenic, in order to allow the digestion of solid food and storing excess energy as fat (Herrera and Amusquivar, 2000). In addition, the animal must be able to regulate its own body temperature in order to survive away from the nest. In post-natal mice, the majority of temperature regulation is generated via non-shivering thermogenesis (NST). NST is dependent on brown adipose tissue (BAT) (CANNON and Nedergaard, 2004). Relatively small increases in *Dlk1* dosage have recently been shown to impair differentiation of BAT. This means that NST does not occur properly, which in turn has a large impact on neonatal survival (Charalambous et al., 2012). This suggests that correct levels of *Dlk1* expression are very important for maintaining normal development; in mammals, this is achieved by imprinting. Many imprinted genes have been shown to regulate postnatal metabolic processes and have effects on mammalian physiological and metabolic adaptations (Charalambous et al., 2007).

Pregnancy is a time of massive metabolic change, with the female being able to adjust her own metabolism to maintain a constant supply of nutrients to the fetus even with changing food availability. It has been demonstrated that in the lead up to birth there is a large increase in levels of secreted DLK1 protein circulating in the mother's blood (Bachmann et al., 1996). Recently, it has been shown that secreted DLK1 protein in the mother's circulation is derived from the developing embryo (Cleaton et al., 2016). It was then demonstrated that the maternal expression of *Dlk1* was required in order to interpret the metabolic signal of the fetal DLK1. This is a highly mammalian-specific process of signaling between the conceptus and the mother with the use of a gene regulated by imprinting (Cleaton et al., 2016).

1.5.2 *Dlk1* is regulated as part of the *Dlk1-Dio3* imprinted cluster

In mouse, *Dlk1* is located within the *Dlk1-Dio3* imprinted cluster on chromosome 12, which is controlled by the intergenic differentially methylated region (IG-DMR) (de Rocha et al., 2008). It is expressed from the imprinted paternal chromosome, and transcription is repressed on the maternal chromosome due to the unmethylated IG-DMR (Edwards et al., 2008). *Dlk1* is dosage-sensitive and if imprinting is removed, effectively resulting in a double dose, it leads to high levels of lethality and tissue-specific growth enhancement, with reciprocal levels of growth retardation in *Dlk1*-null mice (da Rocha et al., 2009; Moon et al., 2002).

The fact that *Dlk1* is part of an imprinted cluster and regulates BAT development, expression throughout all the mammalian-specific extra embryonic tissues, as well as circulating DLK1 derived from the conceptus, suggests that it has been co-opted into numerous mammalian specific processes.

1.6 *Dlk2* in mouse

Dlk2 was first described in 2007 when a detailed search looking for similar genes to *Dlk1* was performed on the published mouse genome (Nueda et al., 2007). It was found to have a similar sequence and protein structure to *Dlk1* (described in Section 1.1). Analysis of the *Dlk2* sequence in mouse and its comparison to other vertebrates suggests that *Dlk2* is much better conserved across the phylum and is potentially the ancestral form from which *Dlk1* arose (C. Edwards pers. Comm., discussed in Section 1.1). Very little is known about the function of *Dlk2*. In the study by Nueda *et al.* in which it was originally described, 3T3-L1 pre-adipocytes, known to be regulated by *Dlk1* (Section 1.4.1), were transfected with expression constructs expressing the sense or anti-sense orientation of *Dlk2*. This study suggests that over-expression of *Dlk2* does not affect differentiation of the pre-adipocytes, but expression of the anti-sense orientation *Dlk2* leads to a decrease in mature adipocyte markers. The authors suggest that this implicates *Dlk2* as a regulator of adipogenesis (Nueda et al., 2007). However, the authors provide no evidence that the expression of the anti-sense *Dlk2* leads to a reduction in DLK2 protein, and has no effect on the levels of other genes, such as the similar sequence of *Dlk1*. It is therefore not possible to draw conclusions about the function of *Dlk2* from this study. The project described in this thesis will be a first study of the function of endogenous *Dlk2* in an *in vivo* system.

1.7 Known mechanisms of *Dlk1* and *Dlk2* function.

1.7.1 *Dlk1* and *Dlk2* as regulators of the Notch signalling pathway

Dlk1 and *Dlk2* contain an EGF-like tandem repeat motif shared with classic Notch ligands. However, as previously described in Section 1.1, they lack domains thought to be essential for interaction with Notch receptors; their intracellular domain is truncated and their DSL domain is entirely lacking (Fig. 1A). This would suggest that *Dlk1* would have lost its ability to act as a Notch ligand. However, evidence from yeast two-hybrid experiments suggests that *Dlk1* interacts with Notch through its EGF-like repeats (Baladrón et al., 2005). Furthermore, when murine *Dlk1* is expressed in *Drosophila,* it acts to inhibit Notch signaling, whereas the typical mouse Delta ligands *Dll1* and *Dll4* are able to activate *Drosophila* Notch signaling (Bray et al., 2008). This suggests that it is possible that *Dlk1* can mediate the Notch signaling pathway despite its lack of functional domains. Further evidence of *Dlk1* mediating Notch signaling is in the examination of *Dlk1* and its ability to promote neurogenesis of neural progenitors derived from ESCs (Surmacz et al., 2011). They show that the over-expression of *Dlk1* leads to higher levels of differentiation in the ESC-derived neural progenitors. When they compare Notch signaling between the control and the *Dlk1*-overexpression cell populations, they see a decrease in downstream Notch targets (Surmacz et al., 2011). However, they demonstrate that the control and the *Dlk1* treatment group have different cell compositions; therefore, the changes in Notch signaling could be due to the relative expression of downstream Notch targets in the different cell populations, rather than a direct result of *Dlk1* signaling. The examination of *Dlk1* or *Dlk2* function through Notch signaling has not been examined properly in an *in vivo* endogenous system.

1.7.2 *Dlk1* as a regulator of non-Notch dependant processes

While the evidence that *Dlk1* operates through Notch signalling is yet to be conclusively shown, it is clear that *Dlk1* can also operate through non-Notch signalling pathways. A study using the 3T3-L1 pre-adipocyte cell line, which demonstrated the role of *Dlk1* inhibiting differentiation of pre-adipocytes, convincingly showed that *Dlk1* directly and in a dose-dependent manner regulated the MEK/ERK pathway (Kim et al., 2007). This study also used mouse embryo fibroblasts (MEFs) derived from *Dlk1*-null mice, demonstrating that these mutant MEFs did not have phosphorylated ERK1/2, enhancing their ability to perform adipogenesis. Upon treatment with the recombinant secreted isoform of DLK1, ERK1/2 was phosphorylated and MEF adipogenesis was inhibited (Kim et al., 2007).

The study which investigated the roles of secreted and membrane-bound DLK1 in NSC regulation in the adult SVZ (Section 1.4.4) assessed if any of this signaling occurs through Notch-dependent pathways. The wild-type NSCs treated with DLK1 were examined for changes in downstream Notch targets, but no change was observed in Notch activity (Ferrón et al., 2011). This study did not examine all downstream Notch targets, so it is possible it is still a Notch mediated process. However, this evidence suggests that the recombinant DLK1, representative of the secreted form of DLK1, was not regulating NSC differentiation through the Notch signaling pathway.

1.8 Zebrafish as a model system for examining *dlk1* and *dlk2* function

In order to examine the mechanisms by which *dlk1* and *dlk2* function, it is important to use an *in vivo* system with endogenous versions of the genes. As demonstrated throughout the Introduction, murine *Dlk1* signals can potentially interact with signalling pathways in three different ways: autocrine, paracrine and endocrine. Therefore, *in vitro* systems, in which cells are isolated from their developmental context, might not fully replicate the more complex interactions with *Dlk1*. The zebrafish provides an ideal model system to examine *dlk1* and *dlk2* as it only contains a single copy of each of the two genes and *dlk1* in zebrafish lacks the juxtamembrane cleavage site (Section 1.2). This suggests that zebrafish *dlk1* will be unable to encode the secreted isoforms of Dlk1 protein, allowing for a model to examine the membrane-bound function of this protein without the complication of its secreted functions. In this section, the aspects of zebrafish development that will be further examined in this thesis are introduced.

1.8.1 Zebrafish embryonic stages

Embryonic stages of zebrafish that are described in this thesis are divided into the developmental stages outlined in a zebrafish staging series paper (Kimmel et al., 1995). The embryos examined in this report are post-gastrulation and are organised into the following categories depending on the hours post fertilisation (h.p.f.):

Segmentation period (10-24 h.p.f.): This period is defined by the development of the somites. During this stage, primary organogenesis occurs. The embryo elongates and the tail bud is rapidly extended.

Pharyngula period (24-48 h.p.f.): Organogenesis continues rapidly throughout the pharyngula period. The body axis straightens, and pigment-containing cells form and limb (pectoral fin) formation is initiated. Circulation begins and the heart starts to beat at the

beginning of this period. This period is subdivided into primordium stages, known as "prim".

Hatching period (48-72 h.p.f.): Hatching of the zebrafish embryos is not always synchronised within a clutch and the stages are defined by hours of development, not by hatching time. This period marks the completion of rapid morphogenesis of many of the organ systems, with some notable exceptions such as the developing gut primordium. Cartilage begins to develop in the head.

Early larval period (72 h.p.f. – 5 d.p.f.): By this stage, morphogenesis is complete and the larva continues to grow rapidly. The swim bladder inflates during this stage and the larva begins to seek food and increasingly responds to stimuli.

1.8.2 Zebrafish neural stem cells in the embryo

In the developing vertebrate brain, the generally accepted model is that before the onset of neurogenesis, the neural epithelium is populated by NSCs. The onset of neurogenesis results in NSCs becoming radial glial cells that will generate all the neurons and then glial cell populations (Paridaen and Huttner, 2014). This model is a basic generalisation and very little is known about the heterogeneity of this radial glial cell population and the way in which they generate neurons throughout development. As a transparent vertebrate embryo, zebrafish is potentially an ideal model to examine the development of these glial cell populations. In the zebrafish embryo, there are a population of glial fibrillary acidic protein (GFAP)-expressing radial glial cells (Johnson et al., 2016). Through fate-mapping of this cell population, it was shown that they generated subsets of interneurons, secondary motorneurons and oligodendroglia cells. In addition, targeted ablation of these cells resulted in the loss of these later born neurons and glial cells, as well as a loss in maintenance of the NSC population (Johnson et al., 2016).

These radial glial cell populations in the zebrafish embryo are regulated by Notch signalling (Appel et al., 2001). In the examination of a *DeltaA* (*dlA*) mutant zebrafish it was discovered that there is a reduction in the proliferative neural cell populations. Supporting the more recent findings of the ablation experiments, these *dlA* mutants had reduced later-born secondary motor neurons and glia (Appel et al., 2001; Johnson et al., 2016). The model suggested in this study is that the radial glial cells that are beginning the process of differentiation express elevated levels of Delta, which increases the Notch signalling in surrounding cells. This maintains the correct levels of self-renewing radial glial cells through the lateral inhibition process often associated with Notch signalling (Appel et al., 2001). Losing Delta in the mutant causes cells to prematurely differentiate as early-born neurons, leading to the loss of the later-born neurons and maintenance of the radial glial cell population (Appel et al., 2001).

1.8.3 Zebrafish adult neurogenic niches and their role in regeneration

Unlike in the mammalian system, zebrafish have an amazing capacity for adult neurogenesis throughout the adult brain. Of particular interest is a population of radial glial cells situated on the periventricular zones of the adult telencephalon (März et al., 2010; Schmidt et al., 2013). These periventricular cells are categorised into three states (Chapouton et al., 2010; März et al., 2010; Schmidt et al., 2013):

1. Quiescent radial glial cells: contain GFAP and high levels of Notch signalling.
2. Dividing radial glial cells: contain GFAP but low levels of Notch signalling.
3. Radial glial cells that express PCNA but no other radial glial markers.

It has been demonstrated that these cells are regulated by the Notch signalling pathway; high levels of Notch activity maintain the radial glial cells as a quiescent population (state 1) and the reduction

of Notch signalling, upon injury, results in the radial glial cells actively dividing and repopulating the damaged area (Chapouton et al., 2010; Kroehne et al., 2011).

1.9 Aims

The studies performed to date on *Dlk1* in the mouse raise a series of questions regarding the relationship between the membrane-bound and secreted isoforms of DLK1 protein, the occurring receptor-ligand interactions, and the different isoforms' signaling pathways. Deciphering these questions *in vivo* in mouse is difficult, as it is challenging to modulate the different isoforms separately as they are expressed from the same gene locus. In addition, *Dlk1* has clearly developed many roles within the mammalian system that may complicate understanding its mechanistic function in the *Dlk1*-null mouse. In particular, the secreted DLK1 that behaves as a circulating hormone makes it difficult to identify all of the sites of function. It also makes *in vitro* studies challenging to interpret because they are possibly taken out of the endogenous context of DLK1 protein. Therefore, the ultimate aim of this project is to produce an *in vivo* model to elucidate the mechanism, and potential ancestral mechanisms, by which *dlk1* and *dlk2* genes function.

Aim 1: The first aim of this project was to examine the expression of *dlk1* and *dlk2* in zebrafish development. By doing so, the aim was to understand the function that *dlk1* and *dlk2* play in zebrafish development, but most importantly, to identify model systems, such as specific organs or developmental events, in which to examine the mechanism by which these genes function.

Aim 2: To understand the effect of modulating *dlk1* and *dlk2* expression *in vivo*. These genes are known to be highly dosage sensitive in the mouse. Therefore, gene function was investigated using available knockdown techniques to reduce the protein levels and examine their *in vivo* function.

Aim 3: To produce and characterise *dlk1* and *dlk2* mutant zebrafish to be used as a model system for elucidating their mechanistic function.

Aim 4: To examine the *dlk2* mutant produced as part of the zebrafish mutation project with particular focus on the model systems identified in aim 1. The ultimate aim was to use this system to understand the mechanism by which *dlk2* functions in zebrafish.

2. Materials and methods

2. Materials and Methods

2.1 Fish maintenance and handling

Fish were maintained under standard conditions, as previously described (Westerfield, 1995), on a 14-hour light and 10-hour dark cycle. Embryos, obtained from natural spawning, were reared in embryo medium (E3M) (5 mM NaCl, 0.17 mM KCl, 0.33 mM$CaCl_2$, 0.33 mM Mg_2SO_4, 5 mM HEPES), allowed to develop at either 25°C or 28°C, and were staged according to established criteria (Kimmel et al., 1995) before fixing in PFA.

2.2 Fin clipping, DNA extraction and genotyping

Adult zebrafish were anaesthetised by immersion in 150 mg/L tricaine, briefly removed from the media. A small piece of tail fin tissue was removed and placed in a microfuge tube and stored at 20°C prior to DNA extraction. 25 uL of lysis buffer (25 mM NaOH with 0.2 mM EDTA) was added to tail fins or whole embryos in individual tubes and incubated at 95°C for 30 mins. 25 uL neutralisation buffer (40mM Tris-HCl) was added, samples were mixed by vortexing and then either used immediately or stored at -20 °C. Genotyping was performed using a custom genotyping assay (KASPAR genotyping assay, LGC genomics) using fluorescent primers designed to the wild-type and mutated DNA sequence. (The KASP assay primers were designed to the following sequence to detect mutation: TAAACATTGTRGATTTTGAYTTCATGTTAAAAGACMGTGACTCTTTCCGC[A/T]GA TGTTTACGTGTGCTCCAGACAGCAGCCGTGTCATAACGGGRCCACTTG) Genotyping assays were run on a Roche LightCycler II 480 and analysed using the endpoint genotyping software.

2.2 Zebrafish Microinjections

Zebrafish microinjections were conducted on one-cell stage embryos using pulled glass capillaries (Harvard Apparatus GC100F-10), pulled using a Sutter Instrument Company Model P-2000 needle puller. One-cell stage embryos were lined up on a glass slide and injected through the yolk into the cell using an Intracel Picospritzer® III running on 70 psi. Injection volume was calibrated by measuring the size of injection volume in mineral oil using a Zeiss Stemi 2000 microscope with W-PI 10x/23 eyepiece reticule. Injections were controlled in the following ways. First, for every MO injection, a control injection (Danieau's solution) and a mismatch MO injection at the same volume/concentration were performed in the same clutch. This was to ensure that all injected embryos would be developmentally matched, and so that controls could be compared with MO injected fish. Second, for every injection a portion of embryos was left uninjected and examined to ensure that embryos were of high quality. If uninjected embryos had high percentage of defects, injected fish were discarded and not analysed further. Morpholino oligonucleotides (MO) were generated by GeneTools LLC Morpholinos (*Dlk2* MO: 5-GCAGCAGAACGACAGCGAGTTTCAT-3, Mismatch control: 5-GCACCACAAGGACAGCCACTTTCAT-3). Following injections, embryos were stored at 28.5 ^{o}C in the dark in a Binder KB53 heating/cooling incubator until 7 hours post-fertilization (h.p.f., hours post-fertilization at 28.5^{o}C) before they were cleared of dead and unfertilized eggs, and then returned to incubate at 28.5^{o}C in the dark.

2.3 Zebrafish Processing

2.3.1 Embryo Fixation

Embryos were staged by morphology and at the desired stage of development, anesthetized with an excess of Ethyl 3-aminobenzoate methanesulfonic acid (Tricaine) and fixed while rocking in either 4% PFA in PBS or Dent's fixative (20% DMSO 80% Methanol). Fish were fixed overnight at 4°C, after which PFA-fixed fish were rinsed out three times in PBS for 10 minutes and two times in methanol for 10 minutes. Fish fixed in Dent's fixative were rinsed in methanol twice for 10 minutes each. All fixed fish were stored in methanol at -20°C for long term storage.

2.3.2 Cryostat Sectioning

Embryos previously fixed in 4% PFA at desired developmental stages were rehydrated from methanol in a series of five minute rinses to PBS (50% PBS/50% methanol, 75% PBS/25% methanol, 90% PBS/10% methanol, 100% PBS). Rehydrated embryos and whole mount immunostained embryos were then incubated in 30% sucrose in PBS at 4°C overnight, and then mounted in Tissue-Tek O.C.T. embedding medium and frozen at -30°C. Embryos were then sectioned at 10 nm using a Bright 5030 Cryostat and collected on Thermo Menzel-Gläser Superfrost Plus slides, which were dried at room temperature for 10 minutes before storage at -20°C. Embryos were mounted to obtain coronal sections of the zebrafish brain. Only sections containing one or both lenses of the eyes were used for analysis to ensure that sections between different fish were anatomically matched.

2.3.3 mRNA Harvesting

For each mRNA sample, one hundred zebrafish at the appropriate developmental stage were dechorionated, transferred to 1.5 mL Eppendorf tubes on ice and excess liquid was removed. Embryos were then mixed with 350 µL Buffer RLT (Qiagen RNEasy kit) homogenized using 1.0 mm glass beads in a Qiagen TissueLyser LT at 50 Hz for 40 seconds. Homogenized samples were then snap frozen to -80°C, thawed, and then processed following standard protocols with a Qiagen RNEasy kit, summarized as follows:

Homogenized samples were centrifuged through a gDNA Eliminator Column (10,000 rpm, 30 seconds), after which flow-through was saved and mixed with 1 volume of 70% Ethanol. The sample was then mixed, transferred to an RNEasy Column, and spun for 15 seconds at 10,000 rpm. The column was then rinsed with 700 µL RWI solution, two rinses of 500 µL RPE solution, uand then placed in a sterile RNAse free tube. RNA was then eluted in 50 µL of RNAse free double distilled H_2O (ddH_2O).

2.3.4 cDNA Generation

After purification, RNA samples were evaluated by agarose gel electrophoresis (0.8% gel, 0.1 µL SafeView Nucleic Acid Stain, run at 100V for 10 minutes) and spectroscopy using a Nanodrop ND1000 spectrophotometer, then stored at -80 °C. cDNA was generated from RNA samples using an Applied Biosciences High Capacity Reverse Transcription Kit and following standard protocol. In brief, a complete reverse transcription master mix (composed of reverse transcription buffer, dNTP mix, reverse transcriptase, RNAse inhibitor, and random primers) was mixed with an equal volume of prepared zebrafish mRNA, and run through the following temperature steps in a Peqlab Peqstar 96 Universal Gradient Thermal Cycler: 25°C for 10 minutes, 37°C for 120 minutes, 85°C for 5 minutes. cDNA was then stored at -80°C.

2.4 In situ hybridisation

ISH was performed as previously described (Thisse and Thisse, 2008). PCR products were cloned into a TOPO PCR II vector and then *in vitro* transcription was performed using Roche DIG RNA Labeling Kit (SP6/T7) to produce dig-labeled anti-sense and sense RNA probes. (*Dlk1* 1st probe: TGTCCGGCTGGGTTCACTGG, ACCAGCTGCCTGTACCTCAC; 2nd probe: CCGCTATCGTCTTCTTCCAG, CACAGTTTGGTTCTCCAGCA. *Dlk2* 1st probe: AAGAAACGTCTCCGACTCCA, GAAGCCTTCAGGACACAAGC; 2nd probe: AATGCACATGTTCTGGGAAC, AACCTAAGCATCTCATCACA) ISH embryos then had their yolk sac cleared through glycerol washes before whole mount imaging.

2.5 Whole Mount Immunostaining

Embryos previously fixed in either 4% PFA or Dent's Fixative at desired developmental stages were rehydrated from methanol storage at -20°C in rinses to PBS (50% PBS/50% methanol, 75% PBS/25% methanol, 90% PBS/10% methanol, 100% PBS). Rehydrated embryos were then blocked in 10% Goat Serum PBS with 0.1% Tween-20 for 1 hour at room temperature, and then incubated in primary antibody in 10% Goat Serum PBS with 0.1% Tween-20 at 4°C overnight. After incubation in primary antibody, embryos were washed out four times in PBS with 0.1% Tween for ten minutes each, and then incubated in appropriate fluorescent secondary for two hours at room temperature. After incubation in secondary antibody, embryos were again washed four times in PBS with 0.1% Tween for ten minutes each and stored in PBS at 4°C. The following primary antibodies were used: anti-HuC (1:200, Santa Cruz), anti-GFAP (1:4, ZIRC zrf-1), and anti-PHH3 (1:200, Millipore). The following secondary antibodies were used: goat anti-mouse conjugated to Alexa Fluor 488 (1:1000, Invitrogen), goat anti-rabbit conjugated to Alexa Fluor 488 (1:500, Invitrogen).

2.6 BrdU analysis

BrdU labeling was performed as previously described (Westerfield et al., 2009). Embryos were injected with 0.025ng (in 0.52 µl) of *dlk2* MO or mismatch at the 1 cell stage. At 24 h.p.f. and 48 h.p.f., BrdU labeling was performed on the MO, the mismatch and uninjected siblings. The BrdU was allowed to incorporate for 5, 10 or 15 minutes. As there was little difference between these times, a 5 minute incorporation was used for replications.

2.7 Microscopy and image processing

2.7.1 Brightfield imaging

All brightfield images were taken on Axio zoom V1.6 microscope with ZEN 2012 software. Whole mount embryos were embedded in either 3% methyl cellulose in E3 medium or 2% low melting point agarose.

2.7.2 Time-lapse microscopy

In order to produce time-lapse films of the developing embryos, they were embedded in 2% agarose and 0.016% tricaine (3-amino benzoic acid ethylester) in E3 medium. The embryos were then imaged using an Axio zoom V1.6 microscope with ZEN 2012 software. The embryos were maintained at 28^{o}C using a heated stage.

2.7.3 Confocal imaging and processing

Confocal images were captured Nikon Eclipse C1si. Embryos were embedded in 2% low melting point agarose onto a slide cover. The slide covers were suspended on a slide holder that allowed them to be imaged on the upright confocal. Wild type embryos were always imaged first and the settings were reused for the treatment groups. Z-stack images were processed in image J, maximum intensity projects were made with no further processing.

2.8 CRISPR-cas9 Guide RNA

The guide RNA sequences were cloned into pDR274. (Target sequences. *Dlk1:* GGCGAGTGTATCTGTGAGTCCGG, GGCGGGCGATGCGTCCGGCGTGG. *Dlk2:* GGCAGGTGTGATCCGGGATGGGG, GGCAGTGCTCCTGCATGGACGGG*)* The guide RNA and the Cas-9 RNA were *in vito* transcribed using the mMessage machine Ultra T7 kit (Invitrogen). The 25pg of guide RNA and 300pg of Cas9 RNA were injected into the one-cell embryo.

2.9 Behavioural Tracking

Tracking equipment was from Zanticks LTD. A 24 well plate was placed in a dark Perspex box and monitored by a camera. Proprietary software was used to track individual fish movements over time. Single larval fish were placed in each well and allowed to acclimatise for at least 1 hour before tracking began.

3. Analysis of the expression patterns of *dlk1* and *dlk2* during early development and in the adult brain of zebrafish.

3.1 Introduction

To understand the expression dynamics of *dlk1* and *dlk2* in the developing zebrafish, a spatio-temporal analysis was performed using mRNA *in situ* hybridisation. To date, there is no published data on the expression of these genes in zebrafish; however, there is detailed analysis of murine *Dlk1* during mouse development (da Rocha et al., 2007; Yevtodiyenko and Schmidt, 2006). In addition, as described in section 1.4.4., murine *Dlk1* plays an essential role in the regulation of neural stem cells within the subventricular zone in the adult mouse (Ferrón et al., 2011). Zebrafish maintains multiple neurogenic niches in the adult brain, which, if regulated by *dlk1* or *dlk2,* could provide an ideal model system to examine the mechanism by which these genes regulate stem cell niches (Chapouton et al., 2011). Therefore, in addition to describing the developmental expression pattern of *dlk1* and *dlk2*, an analysis of the expression of these two genes in the adult brain was performed. mRNA *in situ* hybridisation (ISH) and immunohistochemistry (IHC) techniques were used to address the following aims:

1. To compare and contrast the expression of murine *Dlk1* with zebrafish *dlk1* and *dlk2* to explore the evolutionary conservation of the developmental expression of these genes.
2. To understand the expression of *dlk2* in the context of notch signalling pathways.
3. To identify optimum regions of expression for examination within *dlk2* knock-down and knock-out approaches.

3.2 Results and discussion

3.2.1 *dlk1* is ubiquitously expressed during the segmentation phase of zebrafish embryonic development.

Using *in situ* hybridisation, the expression pattern of *dlk1* was investigated from the post-gastrulation bud phase (10 h.p.f.). This marks the beginning of the segmentation phase of embryogenesis, which includes the completion of somitogenesis and neurogenesis (Kimmel et al., 1995). This phase ends at around 24 h.p.f., coinciding with the completion of somitogenesis. *Dlk1* is ubiquitously expressed in the 10 h.p.f. embryo body (Fig. 3.1A and B). Figure 3.1A shows a lateral view of the embryo and Figure 3.1B shows a dorsal view to demonstrate clear expression throughout the developing neural epithelium. This ubiquitous expression is maintained throughout the segmentation phase, and continues to be expressed throughout the 18 somite (~18 h.p.f.) zebrafish embryo (Fig. 3.1C and D).

The ubiquitous expression of *dlk1* in the early zebrafish shares some similarities with the expression of *Dlk1* in early stages of murine development. At E10, murine *Dlk1* is broadly expressed in the mouse embryo before becoming increasingly localised to specific locations later in development (da Rocha et al., 2007). In mouse, *Dlk1* is expressed throughout undifferentiated mesenchyme. This tissue is comparable to the pre-somitic mesoderm in zebrafish, in which *dlk1* is expressed throughout the segmentation period (Fig. 3.1). Murine *Dlk1* is also expressed in the developing retina, and shows expression in the optic primordium and optic vesicle of the bud-stage and 18–somite-stage zebrafish, respectively. However, murine *Dlk1* is only expressed in specific ectodermal tissues at this stage in development, such as the optic chiasm, Rathke's pouch and the developing pituitary gland. Zebrafish *dlk1* is expressed throughout the ectodermal tissues, as well as all mesodermal tissue.

3.2.2 *dlk1* expression becomes increasingly restricted to anterior domains by the pharyngula stage of embryonic development.

The pharyngula stage of zebrafish development marks the continuation of organogenesis, with the formation of many of the major organs. *Dlk1* maintains a broad domain of expression at this stage

of zebrafish embryonic development. At 25 h.p.f. zebrafish have strong *dlk1* expression throughout the brain, including the forming telencephalon, optic tectum, cerebellum, rhombencephalon and developing retina (Fig. 3.2A and B). These 25 h.p.f. embryos also show lower expression of *dlk1* in the developing trunk relative to the anterior neuronal regions. However, expression is maintained at these low levels in these mesodermal tissues throughout the pharyngeal stage, from 25 h.pf to 42 h.pf. (Fig. 3.2 A-F). At the end of the pharyngula stage development (42 h.p.f.), *dlk1* expression can be seen in some endodermal tissues such as the liver and forming gut primordium (Fig. 3.2E).

The murine E12.5 embryo maintains a much higher expression of *Dlk1* in the mesodermal tissues relative to the ectoderm. Unlike the expression pattern observed in zebrafish, murine *Dlk1* is never expressed in such a broad manner in ectodermal tissue, being constrained largely to the developing pituitary gland, hypothalamus and optic recess (da Rocha et al., 2007). Murine *Dlk1* has very strong expression in endodermal tissues at E12.5, particularly in the liver, which is also observed in the developing zebrafish.

3.2.*3 dlk1* expression is constrained to neuronal regions during the hatching stage of embryonic development.

The hatching stage is a period of rapid morphogenesis and occurs from 48 h.p.f. to 72 h.p.f. Most of the major organ systems complete rapid morphogenesis by the end of this phase. In the 48 h.p.f. embryo, *dlk1* expression is constrained to the brain (Fig. 3.3A and B). All previous mesodermal expression of *dlk1* has ceased by the hatching stage. The brain has a broad domain of *dlk1* expression throughout from 48 h.p.f. and is maintained in this fashion until 60 h.p.f. (Fig. 3.3 C-F). The 48 h.p.f. zebrafish maintains strong expression in the developing liver (Section ISH performed by Sophie Miller).

In contrast, the E16.5 mouse embryo has very low levels of *Dlk1* in neuronal tissues, becoming constrained to highly specific locations. Additionally, murine *Dlk1* maintains its mesodermal expression to a much higher degree than zebrafish. At this stage, the zebrafish embryo maintains *dlk1* liver expression, much like the mouse.

3.2.4 *dlk1* is expressed in specific neuronal locations in larval zebrafish.

At 72 h.p.f., the zebrafish is a free swimming larvae, able to respond to basic stimuli such as touch and vibration (Kimmel et al., 1995). By 72 h.p.f., *dlk1* has become constrained to specific regions of neuronal tissues (Fig. 3.4A). The larval zebrafish have high expression in specific regions of the optic tectum and medulla oblongata. However, *dlk1* is still expressed throughout the larval brain as well (Fig. 3.4A). This expression pattern is maintained up until 5 d.p.f. (Fig. 3.4 C-D).

Postnatal mice have very limited expression of *Dlk1*, and its expression becomes increasingly restricted in the lead up to birth. In the postnatal mouse brain, *Dlk1* is restricted to the sub ventricular zone, in contrast to the zebrafish larvae which express *dlk1* throughout the brain.

3.2.5 *dlk1* is expressed in radial glial cells in the adult telencephalon.

Since murine Dlk1 is expressed in the neural stem cells of the subventricular zone, a comparative investigation was performed in the adult zebrafish brain using ISH on wax sections. Expression was observed in the peripheral cell layer of the adult telencephalon. The location of the *dlk1* expression closely matched that of the described radial glial cells, shown to be responsible for regeneration upon injury of the telencephalon (Kroehne et al., 2011). The zebrafish radial glial cells in the telencephalon fall into three categories: Type I are quiescent cells waiting for a stimulus to become activated, and Type II are a population of dividing cells that self-renew and differentiate

into Type III cells, which are a transit amplifying cell population. Type I is identified by the co-expression of GFAP and notch signalling, Type II by GFAP and PCNA, and Type III by the expression of PCNA only (Chapouton et al., 2010; März et al., 2010). In order to confirm that the expression of *dlk1* was in these particular cells, *dlk1* ISH was performed in a Her4:GFP transgenic zebrafish, followed by IHC with GFAP and PCNA antibodies. Using these radial glial cell markers, it can be seen that *dlk1* is expressed in the radial glial cell population.

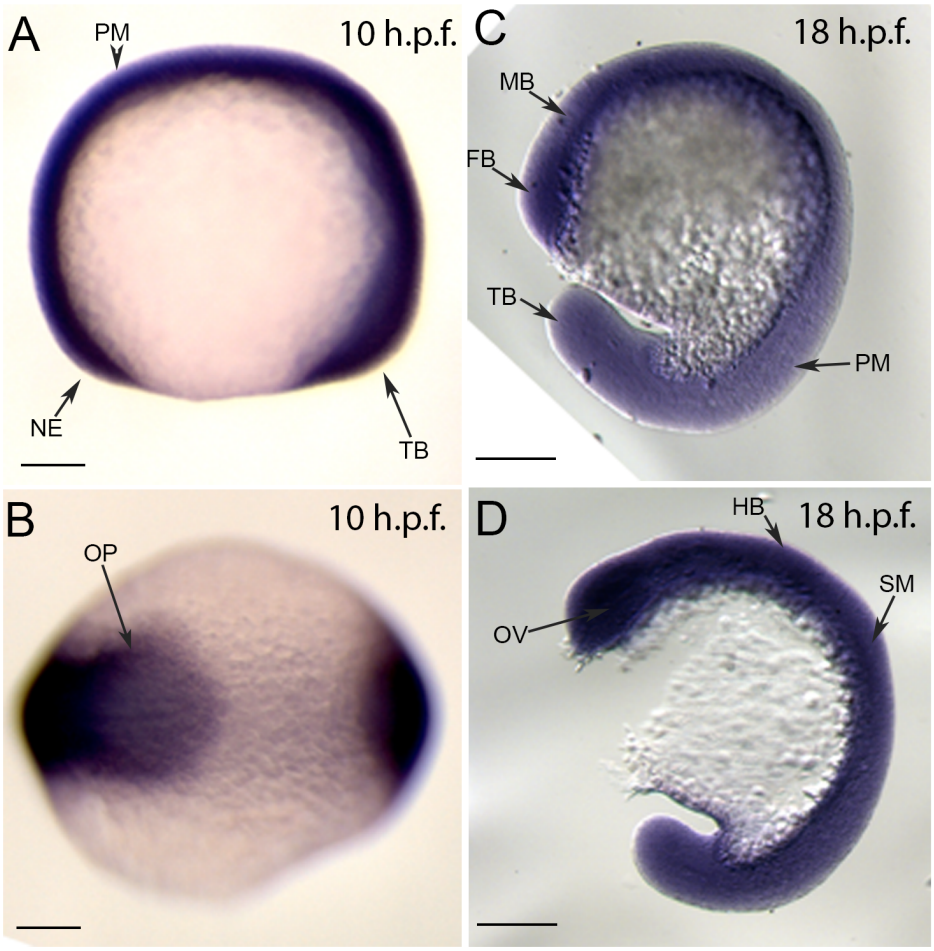

Figure 3.1 | *dlk1* is ubiquitously expressed throughout the segmentation phase of zebrafish development. A, shows a lateral view of dlk1 in situ at the bud stage (10 h.p.f.). B, shows a ventral view of dlk1 in situ at the bud stage (10 h.p.f.). dlk1 is expressed throughout the bud stage embryo. C and D, Show two different representative lateral view images of dlk1 in situ at the 18 somite stage (18 h.p.f.). dlk1 is ubiquitous expressed at the 18 somite. Neural ectoderm (NE), optic primordium (OP), pre-somitic mesoderm (PM), tail bud (TB), optic vesicle (OV), forebrain (FB), midbrain (MB), hindbrain (HB), somitic mesoderm (SM). Scale bar, 0.5mm.

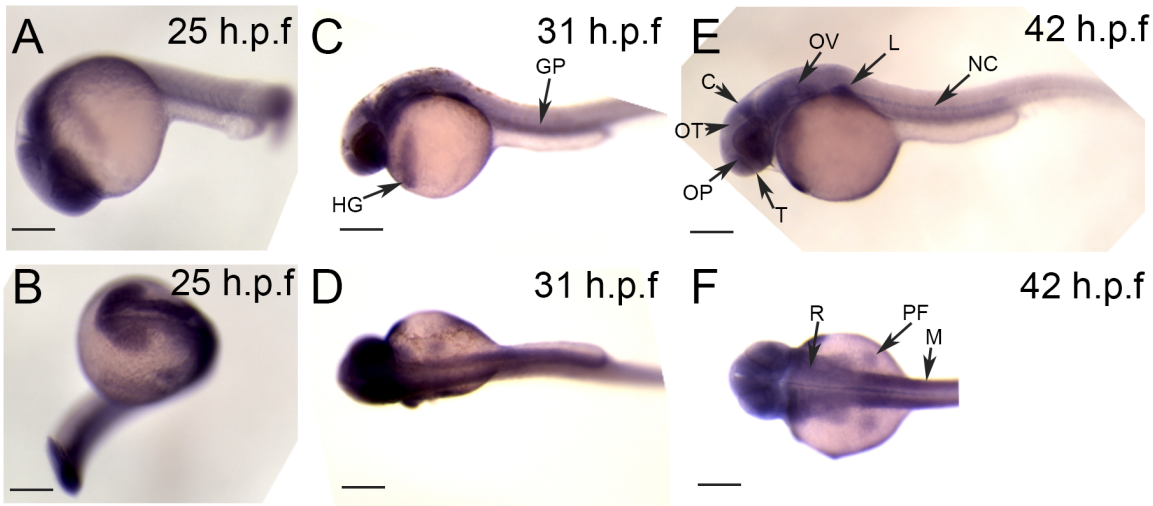

Figure 3.2 | *dlk1* expression becomes increasingly restricted to anterior structures by the pharyngula stage of embryonic development A, shows a lateral view of *dlk1* ISH at the prim-6 stage (25 h.p.f.). B, shows a dorsal view of *dlk1* ISH at the prim-6 stage (25 h.p.f.). At prim-6, *dlk1* is broadly expressed throughout the embryo body. Expression can be seen in the brain and developing trunk and myotomes. C, shows a lateral view of *dlk1* ISH at the prim-16 stage (31 h.p.f.). D, shows a dorsal view of *dlk1* ISH at the prim-16 stage (31 h.p.f.). The broad *dlk1* expression domain is maintained into the prim-16 stage, with stronger expression appearing in the developing gut primordium and hatching gland. E, shows a lateral view of *dlk1* ISH at the high-pec stage (42 h.p.f.). F, shows a dorsal view of *dlk1* ISH at the high-pec stage (42 h.p.f.). At 42 h.p.f. *dlk1* expression remains strong in the brain, but starts to reduce in the trunk. The developing liver becomes a defined tissue and *dlk1* is expressed there. The notochord also has some *dlk1* expression. Hatching gland (HG), telencephalon (T), optic pit (OP), optic tectum (OT), cerebellum (C), otic vesicle (OV), rhombencephalon (R), notochord (NC), pectoral fin (PF), myotomes (M), liver (L). Scale bar, 0.25mm

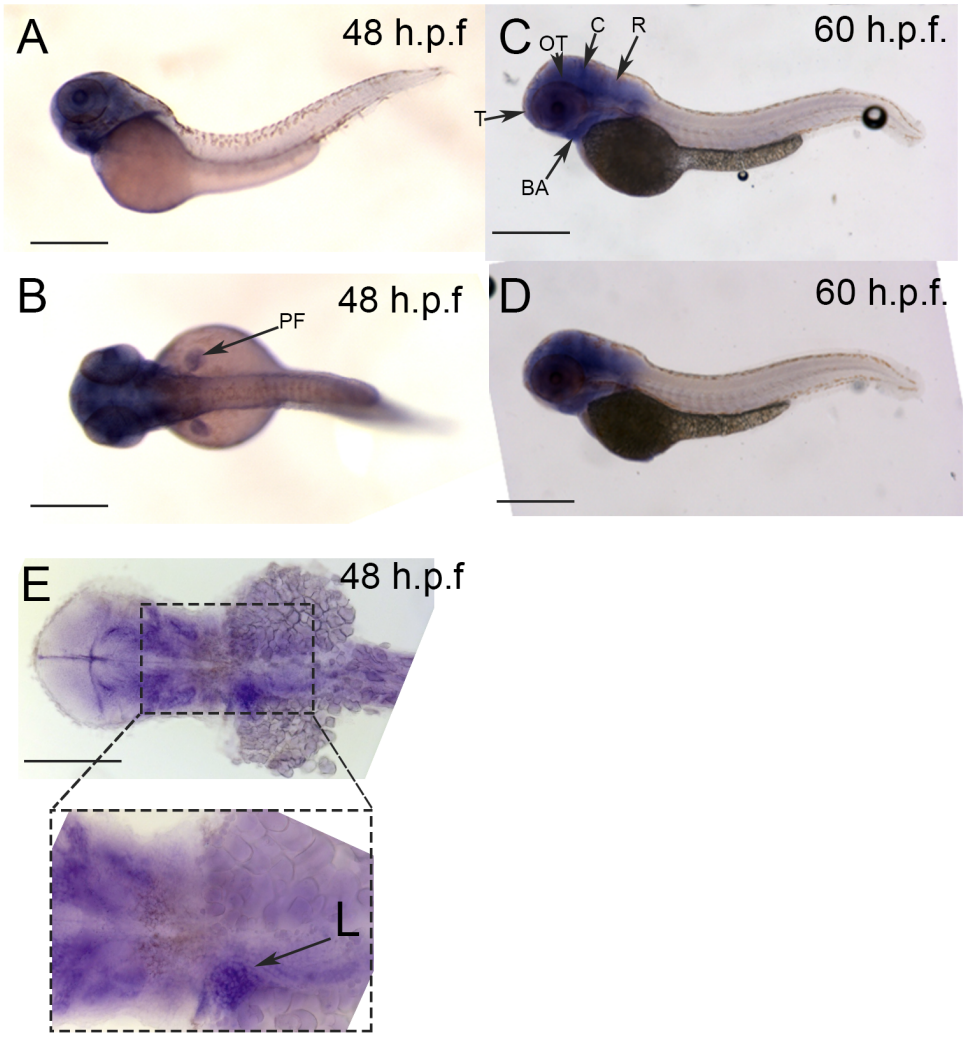

Figure 3.3 | *dlk1* expression is limited to anterior neuronal structures and liver during hatching stage of embryonic development A, shows a lateral view of *dlk1 ISH* at the long-pec stage (48 h.p.f.). B, shows a ventral view of *dlk1 ISH* at the long-pec stage (48 h.p.f.). *Dlk1* expression is observed within the brain tissue, the branchial arches and the developing pectoral fin at this stage. C and D, Show two different representative lateral view images of *dlk1 ISH* at the pec-fin stage (60 h.p.f.). *Dlk1* expression domains at 60 h.p.f. remain consistent with the onsent of the hatching stage, 48 h.p.f. E and F, show a section ISH of *dlk1* in the 48 h.p.f. embryo and a high magnification of the same section respectively. The section ISH demonstrates that *dlk1* is still maintained at the 48 h.p.f. time point and that the broad expression of *dlk1* in the wholemount ISH is not an artefact of probe trapping (Section ISH performed by Sophie Miller). Telencephalon (T), branchial arches (BR), optic tectum (OT), cerebellum (C), rhombencephalon (R), pectoral fin (PF), liver (L). Scale bar, 0.5mm

Figure 3.4 | *dlk1* is expressed in specific neuronal locations in larval zebrafish

A, shows a lateral view of *dlk1* ISH at the protruding mouth stage (72 h.p.f.). **B**, shows a dorsal view of *dlk1* ISH at the protruding mouth stage (72 h.p.f.). Expression of *dlk1* is seen only in the brain region and is absent in the trunk. **C and D**, Show two different representative lateral view images of *dlk1* ISH at the 4-day larval stage. *Dlk1* expression is seen in the brain and also the branchial arches. **E**, shows a lateral view of *dlk1* ISH at the 5 day larval stage. **F,** shows a dorsal view of *dlk1* ISH at the 5-day larval stage. **G**, is a schematic of a dorsal view of the larval zebrafish with a representation of *dlk1* ISH signal. *Dlk1* expression persists in the brain and branchial arches but is absent from all trunk tissues. Telencephalon (T), optic tectum (OT) cerebellum (C) hindbrain (HB) branchial arches (BA) brain stem (BS). Scale bar, 0.5mm

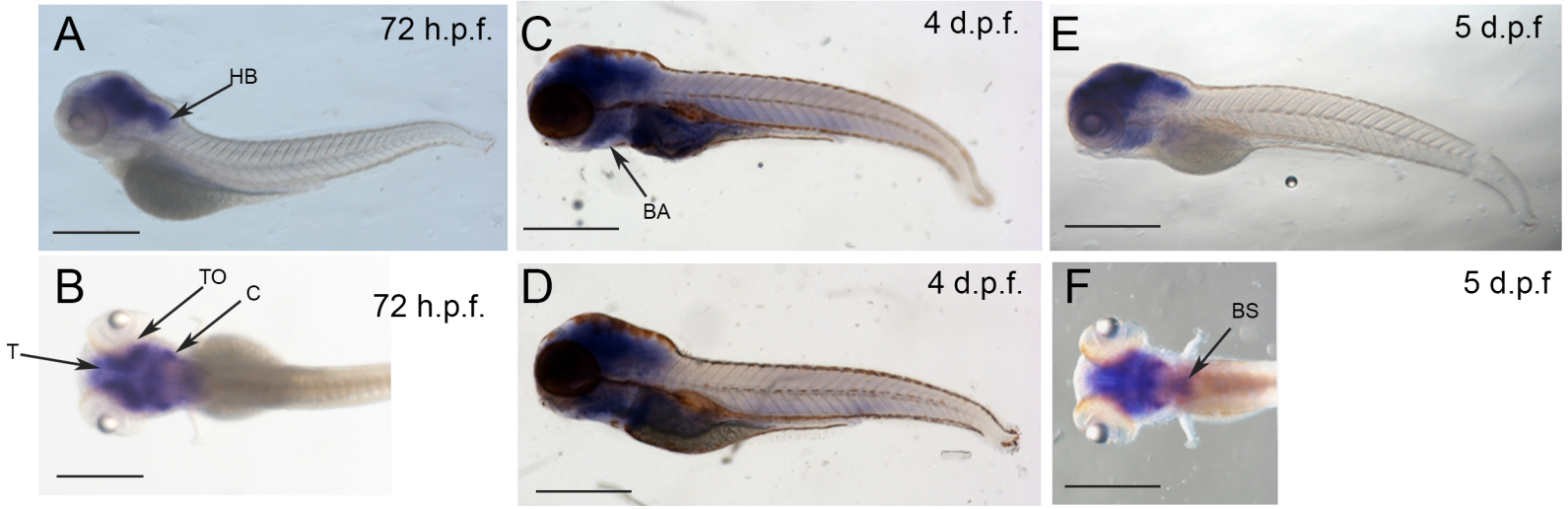
A
72 h.p.f.
HB
C
4 d.p.f.
BA
E
5 d.p.f
B
TO
C
T
72 h.p.f.
D
4 d.p.f.
F
BS
5 d.p.f

G

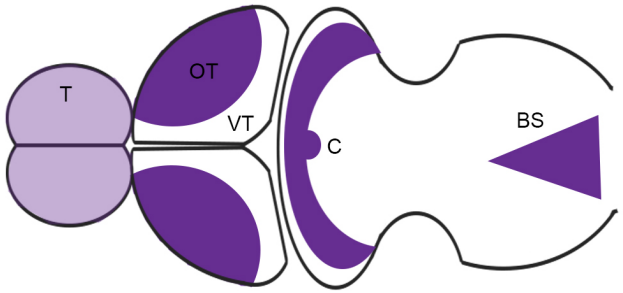
T
OT
VT
C
BS

Figure 3.5 | *dlk1* is expressed in Type I and Type II radial glial cells in the adult telencephalon.

A., schematic representation of a transverse section through the adult zebrafish telencephalon with boxes demonstrating where the rest of the images in the figure are situated. **B.,** Representative image of *dlk2* ISH followed by IHC for PCNA and GFAP, in the context of a her4:GFP transgenic fish (described in materials and methods, section 2.xx). The IHC was performed on the same section with a photo-bleaching step in between each IHC that required the use of the same secondary antibody fluorophore (materials and methods, section 2.xx). **C.,** Demonstrates the presence of *dlk1* in type I radial glial cells, where both *her4* and GFAP are present. **D.,** Demonstrates the presence of *dlk1* in type II radial glial cells, where GFAP is present but *her4* is not.

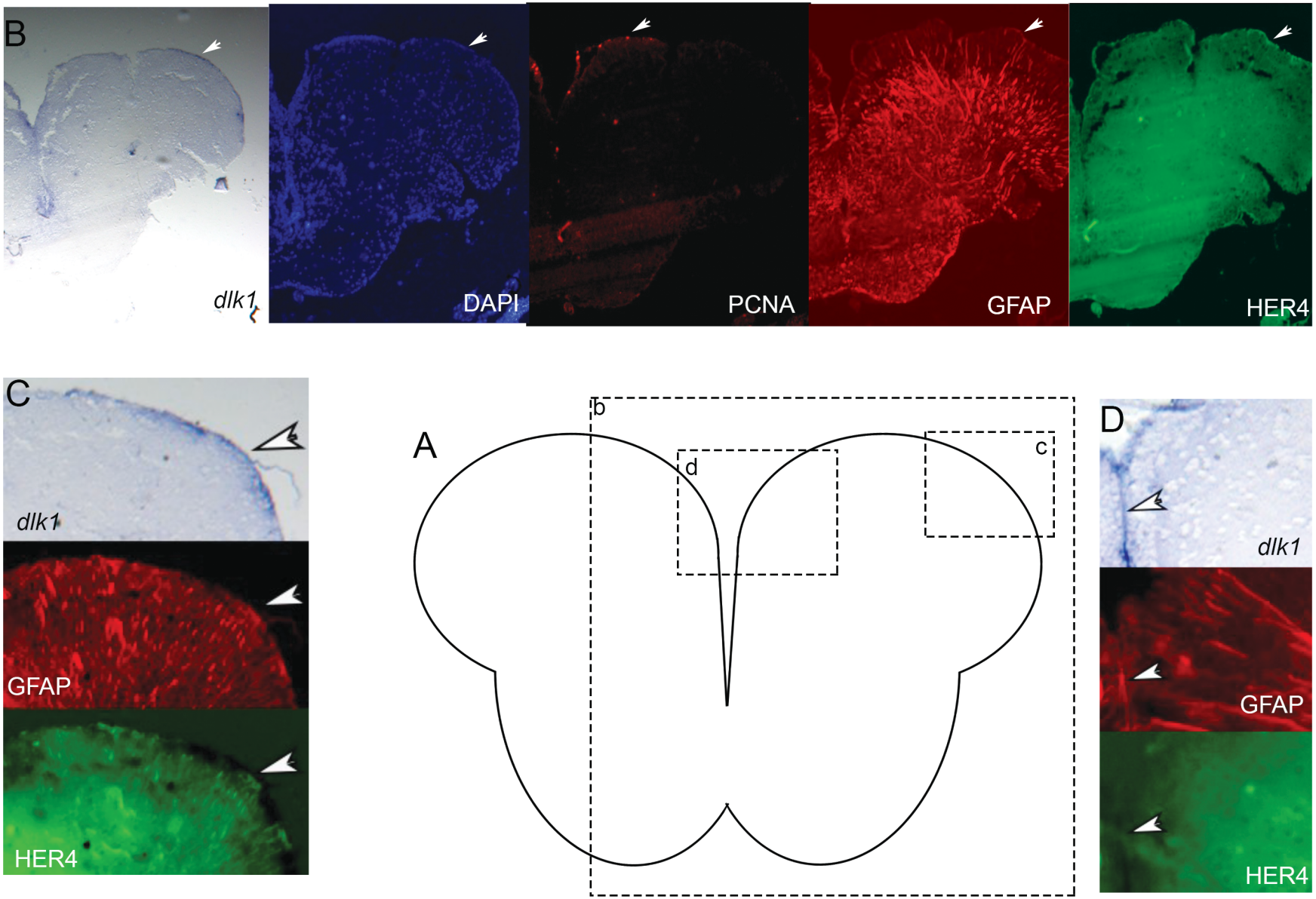
B
dlk1
DAPI
PCNA
GFAP
HER4
C
dlk1
GFAP
HER4
A
b
d
c
D
dlk1
GFAP
HER4

3.2.6 Unlike *dlk1, dlk2* becomes localised to the anterior of the zebrafish embryo during the segmentation phase

ISH of *dlk2* at the segmentation phase of zebrafish development shows that, like *dlk1, dlk2* is ubiquitously expressed at the bud stage of embryonic development (Fig. 3.6A and B). However, by 18 somites, *dlk2* expression is beginning to become localised to the anterior portion of the zebrafish embryo at an earlier stage than *dlk1* (Fig 3.6 C and D). There is still expression in the tail bud and pre-somatic mesoderm, but this is reduced in comparison to the anterior of the embryo and in contrast to *dlk1* expression (Fig. 3.1C and D). The somitic mesoderm retains *dlk2* expression at this stage.

3.2.7 *dlk2* expression becomes localised to anterior neuronal structures by the pharyngula stage of embryonic development.

By prim-6, *dlk2* expression is restricted to the developing brain, earlier then *dlk1* (Fig. 3.7A and B). However, by prim-16, *dlk2* and *dlk1* have very similar and overlapping expression patterns. (Fig. 3.7C and D). This similarity and overlapping of expression is maintained through to the end of the hatching period (Fig. 3.8).

3.2.8 *dlk2* is expressed in specific neuronal locations in larval zebrafish that are distinct from that of *dlk1.*

Dlk2 ISH was performed on larval zebrafish from 72 h.p.f. to 5 d.p.f. (Fig. 3.9). From a lateral view of the zebrafish larvae, *dlk1* and *dlk2* appear to have overlapping expression patterns (Fig.

3.9A and B). Both are expressed in the larval zebrafish brain. However, a dorsal view clearly indicates distinct domains of expression (Fig. 3.9D). *Dlk2* is expressed in the telencephalon midline, the proliferative zone at the extremity of the optic tectum, and the vagal lobe.

3.2.10 DLK2 protein mostly co-localises with *dlk2* expression and is present in domains expressing Notch signalling during zebrafish development

DLK2 antibodies were produced as a result of ongoing collaborations with Abcam. Two DLK2 antibodies were produced and characterised in the laboratory, one against a mouse epitope and another against the full length human recombinant protein. Both are polyclonal antibodies. Neither antibody showed specific staining in western blot analysis (not shown), but specific labelling was observed with the polyclonal human DLK2 antibody. Furthermore, this staining was absent in homozygous *dlk2* mutant zebrafish (described in section 3.1). Whole mount IHC was performed in the context of a Notch transgenic reporter. At segmentation, pharyngula and larvae stages showed DLK2 localisation correlates closely with *dlk2 in situ* expression patterns (Fig. 3.10). This suggests that the antibody is not detecting DLK2 protein within the same tissues/cells that express the *dlk2* mRNA. Therefore, it can be interpreted that either the DLK2 protein it is not secreted in zebrafish or the secreted portion of the protein is not detected by the antibody used.

3.2.11 Dlk2 protein is expressed in cell populations adjacent to those expressing Notch activation markers in the larval brain

To investigate the specific cell populations expressing DLK2 protein, sections of Notch-reporter larval zebrafish, had DLK2 IHC performed on them. The whole mount DLK2 IHC demonstrates that active Notch signalling is occurring within the same domains in which DLK2 is present (Fig.

3.10). However, at high magnification, one can observe that there is no co-localisation between the cells expressing the Notch reporter and those expressing DLK2 at this stage (Fig. 3.11). Instead, DLK2 is present in cells that are adjacent to the cells with active Notch signalling. This suggests that if DLK2 is regulating Notch signalling, it is via trans-regulation not cis-regulation, hinting at possible mechanisms for the functioning of this protein.

3.2.11 Dlk2 protein is present in the radial glial cells in the telencephalon

Dlk2 expression was examined in the adult telencephalon using ISH. Unlike *dlk1, dlk2* never produced any *in situ* signal in the adult telencephalon. By performing Dlk2 IHC on sections of wild type adult telencephalon, signal was found to co-localise with GFAP IHC (Fig 3.12). This demonstrates that Dlk2 protein is localised in the radial glial cell population.

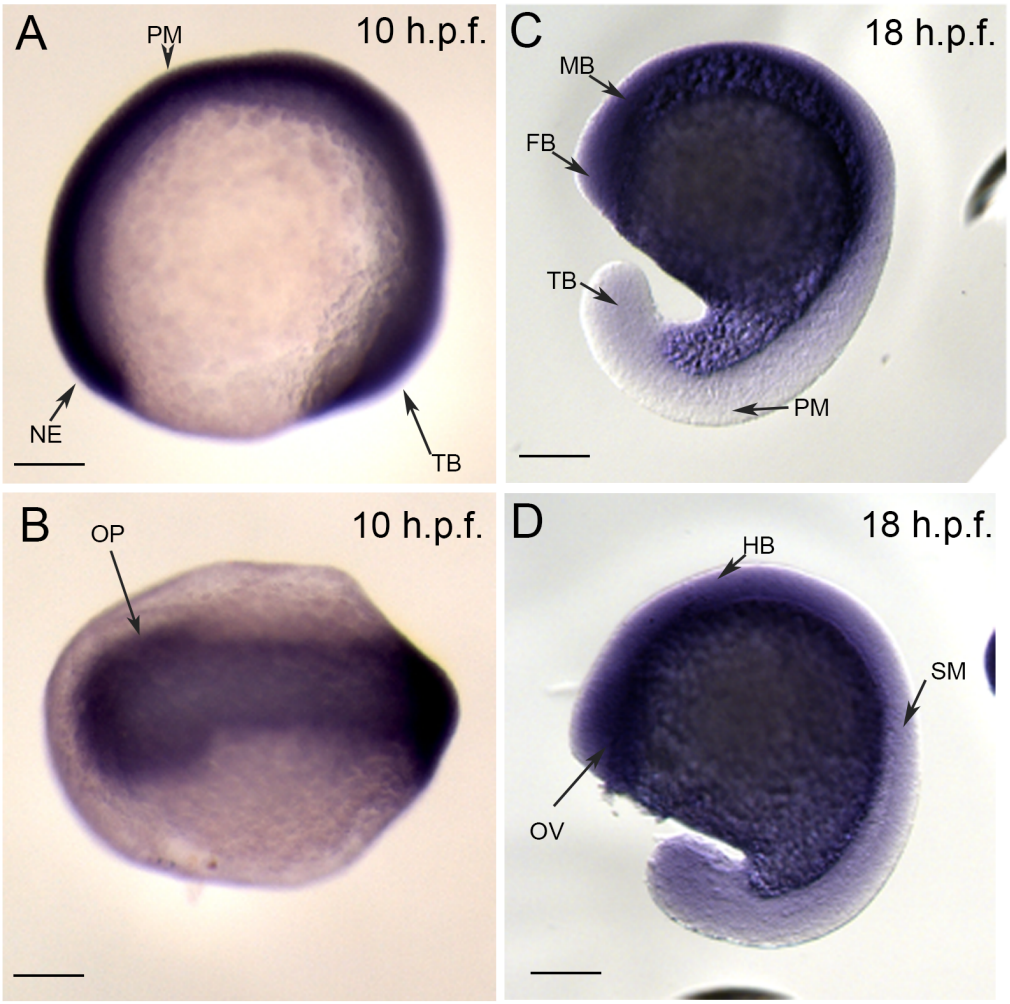

Figure 3.6 | *dlk2* is ubiquitously expressed at the bud stage but becomes more restricted to anterior structures by 18 somites at the end of the segmentation phase of zebrafish development. A, shows a lateral view of *dlk2* in situ at the bud stage (10 h.p.f.).B, shows a ventral view of *dlk2* in situ at the bud stage (10 h.p.f.). C and D, Show two different representative lateral view images of *dlk2* in situ at the 18 somite stage (18 h.p.f.). *Dlk2* maintains a broad domain of expression at this stage, but has reduced expression in the pre-somitic mesoderm and tail bud relative to the brain, in contrast to *dlk1* that maintains ubiquitous expression at this stage. Neural ectoderm (NE), optic primordium (OP), pre-somitic mesoderm (PM), tail bud (TB), optic vesicle (OV), forebrain (FB), midbrain (MB), hindbrain (HB), somatic mesoderm (SM). Scale bar, 0.25mm

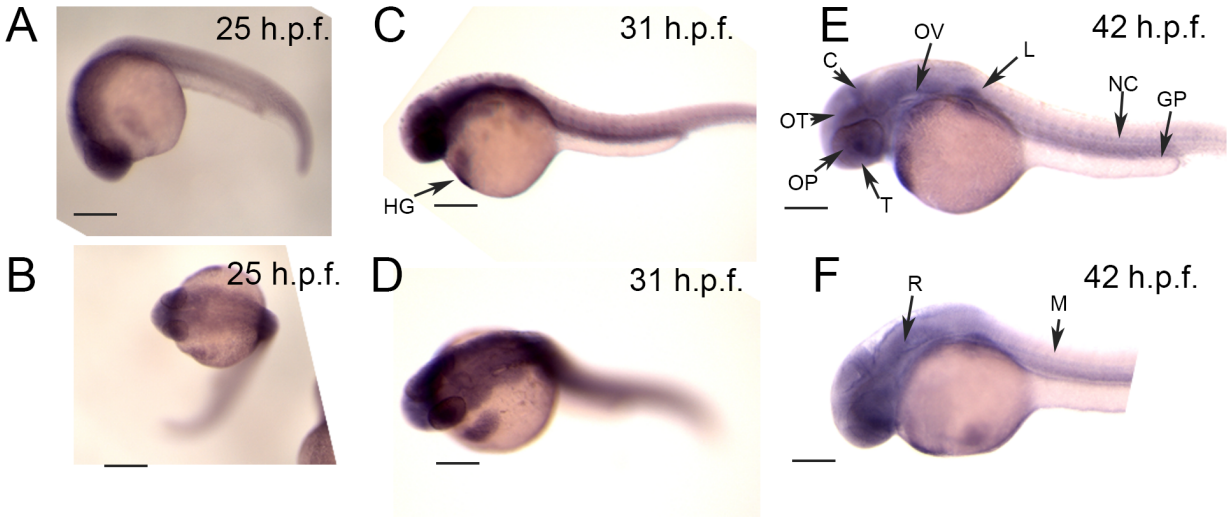

Figure 3.7 | *dlk2* expression is becomes increasingly restricted to anterior structures by the pharyngula stage of embryonic development. A, shows a lateral view of *dlk2 ISH* at the prim-6 stage (25 h.p.f.). B, shows a dorsal view of *dlk2 ISH* at the prim-6 stage (25 h.p.f.). At prim-6, *dlk2* is highly expressed in the anterior structures, such as the brain, but has low expression in the trunk. C, shows a lateral view of *dlk2 ISH* at the prim-16 stage (31 h.p.f.). D, shows a dorsal view of *dlk2 ISH* at the prim-16 stage (31 h.p.f.). The prim-16 expression of *dlk2* remains similar to that of prim-6, however, expression increases in the hatching gland and developing gut primordium. E and F, show two representative images of a lateral view of *dlk2 ISH* at the high-pec stage (42 h.p.f.). At this stage, the *dlk2* expression becomes apparent in the developing liver. Expression is maintained in the anterior structures of the high-pec embryo, with expression also appearing in the notochord but remaining low in the myotome. Hatching gland (HG), telencephalon (T), optic pit (OP), optic tectum (OT), cerebellum (C), otic vesicle (OV), rhombencephalon (R), liver (L), notochord (NC), gut primordium (GP), Myotomes (M). Scale bars, 0.5mm

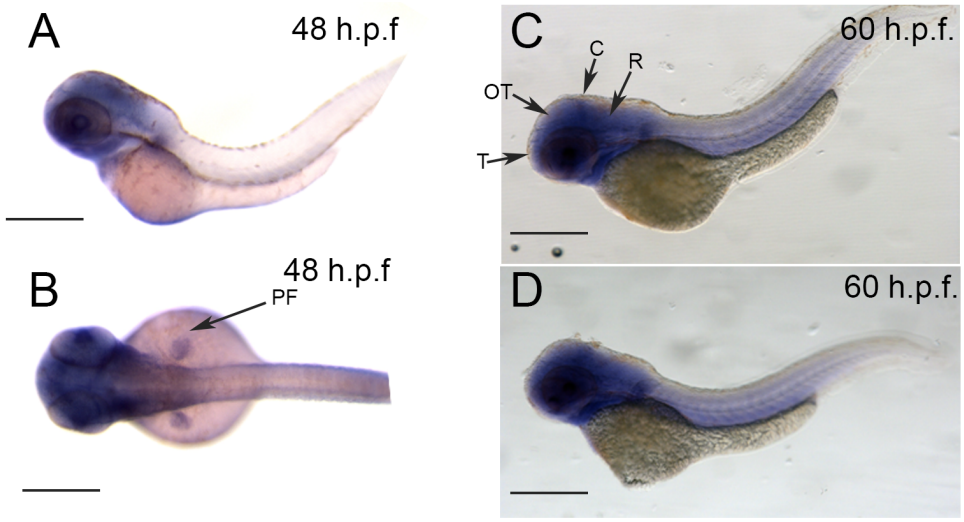

Figure 3.8 | dlk2 expression is limited to anterior neuronal structures and liver during hatching stage of embryonic development. A, shows a lateral view of *dlk2 ISH* at the long-pec stage (48 h.p.f.).B, shows a ventral view of *dlk2 ISH* at the long-pec stage (48 h.p.f.). By 48 hours of development, *dlk2* expression has become highly restricted to the brain, losing expression in the gut and notochord. At this stage the expression becomes apparent in the pectoral fin primordium. C and D, Show two different representative lateral view images of *dlk2 ISH* at the pec-fin stage (60 h.p.f.). The 60 h.p.f. zebrafish embryo maintains the expression pattern of the earlier 48 h.p.f. hatching stage embryo. Telencephalon (T), Optic Tectum (OT), Cerebellum (C), Rhombencephalon (R), Pectoral Fin primordium (PF). Scale bars, 0.5mm

Figure 3.9 | *dlk2* is expressed in specific regions of the larval zebrafish brain.

A, shows a lateral view of *dlk2 ISH* at the protruding mouth stage (72 h.p.f.). **B,** shows a dorsal view of *dlk2 ISH* at the protruding mouth stage (72 h.p.f.). Expression of *dlk2* is seen only in the brain region and is absent in the trunk. **C and D**, Show two different representative lateral view images of *dlk2 ISH* at the 4 day larval stage. In addition to the brain expression, *dlk2* is expressed in the brachial arches. **E,** shows a lateral view of *dlk2 ISH* at the 5 day larval stage. **F,** shows a dorsal view of *dlk2 ISH* at the 5 day larval stage. At this stage, *dlk2* is highly expressed in the brain, with very specific localisation in the midline of the telecehpalon, and the peripheral zones of the optic tectum and cerebellum. **G**, is a schematic of a dorsal view of the larval zebrafish with a representation of *dlk2 ISH* signal, showing the specific regions of *dlk2* expression visable from the dorsal view of a larval zebrafish brain. Telencephalon (T), Optic Tectum (OT) Cerebellum (C) Hindbrain (HB) Branchial Arches (BA) Brain Stem (BS). Scale bars, 0.5mm.

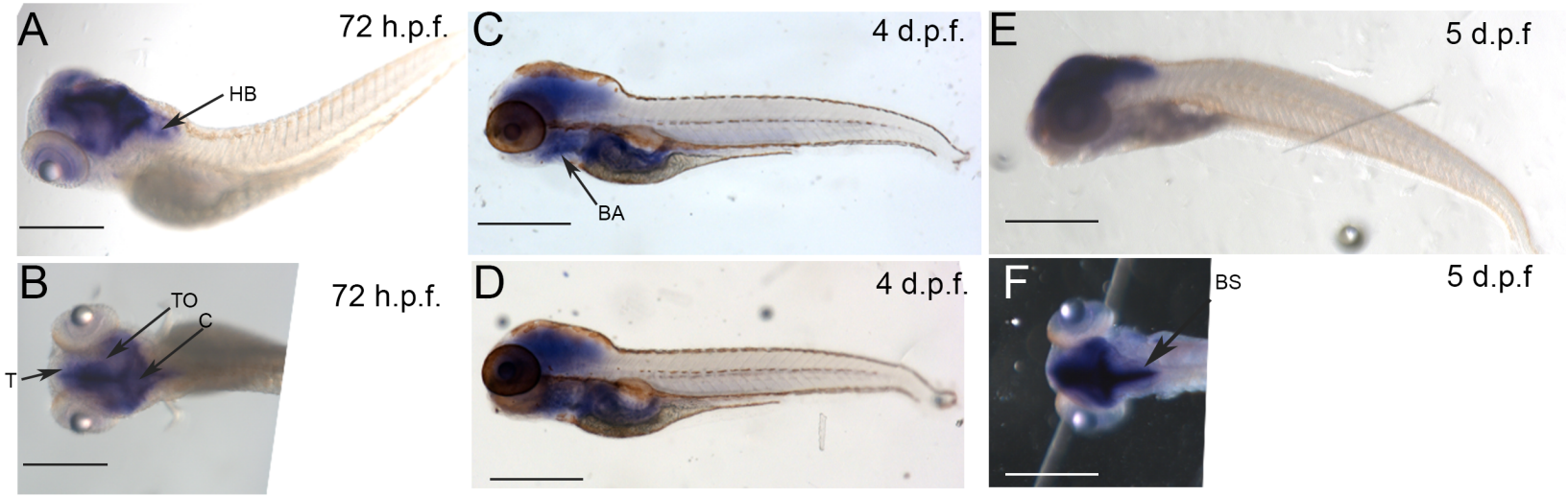
A
72 h.p.f.
HB
C
4 d.p.f.
BA
E
5 d.p.f
B
72 h.p.f.
TO
C
T
D
4 d.p.f.
F
BS
5 d.p.f

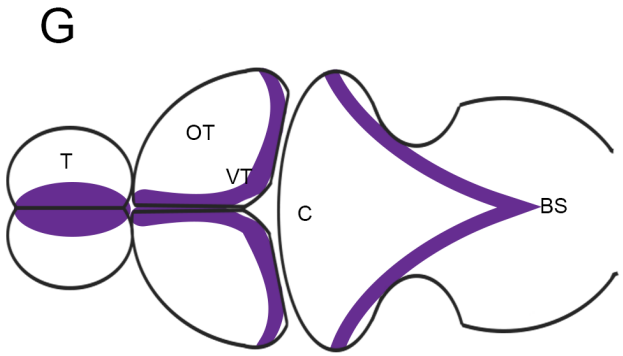
G
T
OT
VT
C
BS

Figure 3.10 | DLK2 is localised to the same regions as the *dlk2 in situ.*

A., Shows DLK2 IHC in the context of the notch reporter transgenic zebrafish at the 18 h.p.f. stage of embryonic development. **B.,** Shows DLK2 IHC performed in the notch reporter transgenic zebrafish at the 24 h.p.f. stage of embryonic development. **C.,** Shows DLK2 IHC performed in the notch reporter transgenic zebrafish at the 5 d.p.f. larval stage. Scale bars, 0.5 mm

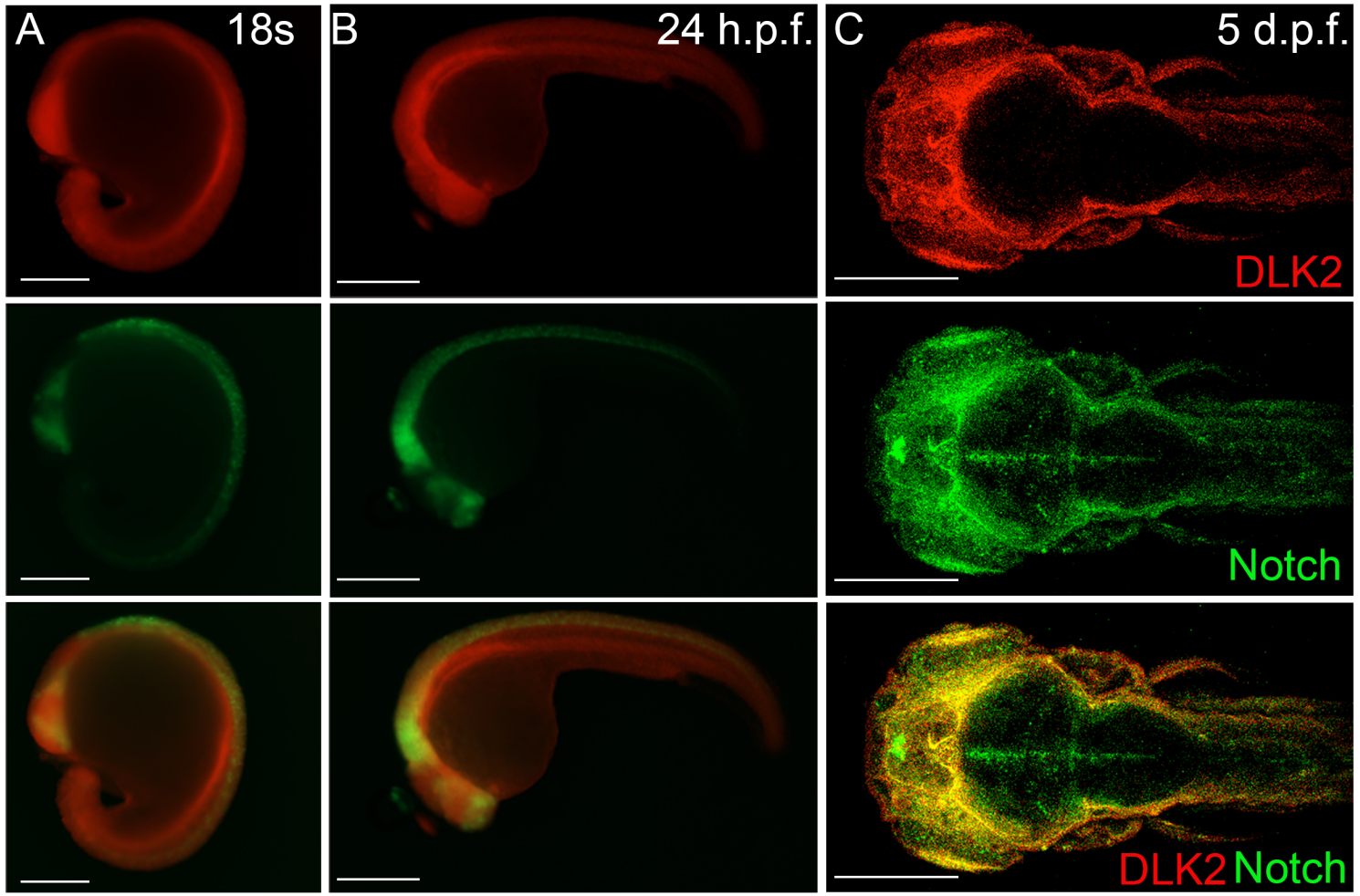
A
18s
B
24 h.p.f.
C
5 d.p.f.
DLK2
Notch
DLK2 Notch

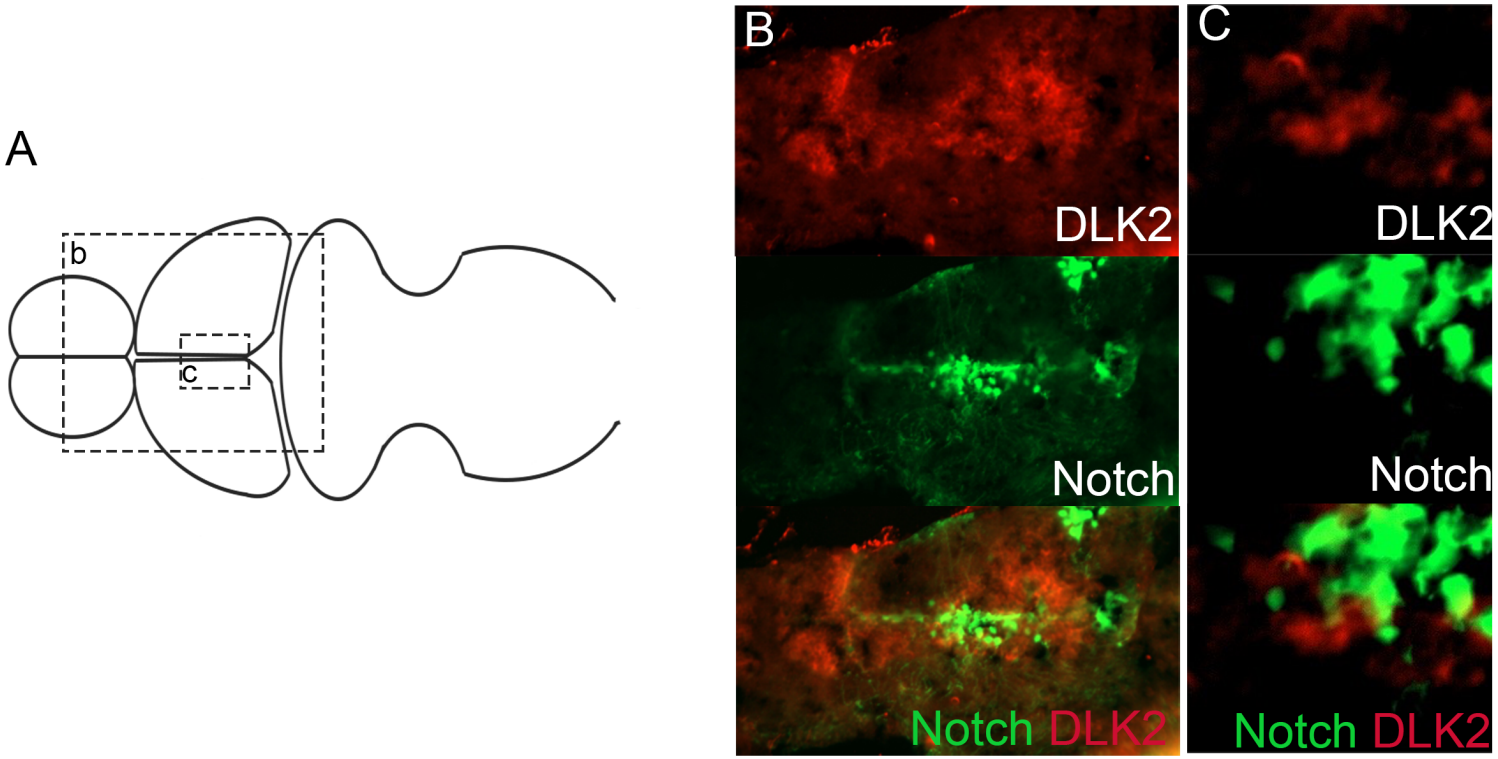

Figure 3.11 | DLK2 in the larval brain is in similar locations to notch signalling but appears to not co-localise and be in adjacent cells. A., schematic representation of the larval brain with boxes demonstrating where the rest of the images in the figure are situated. **B.,** Shows a section of 5 d.p.f. zebrafish brain with DLK2 IHC performed in the context of a notch reporter transgenic zebrafish **C.,** Shows a high magnification maximum intensity projection of some of the cells in this section, demonstrating that the signal is in adjacent cells not co-localised.

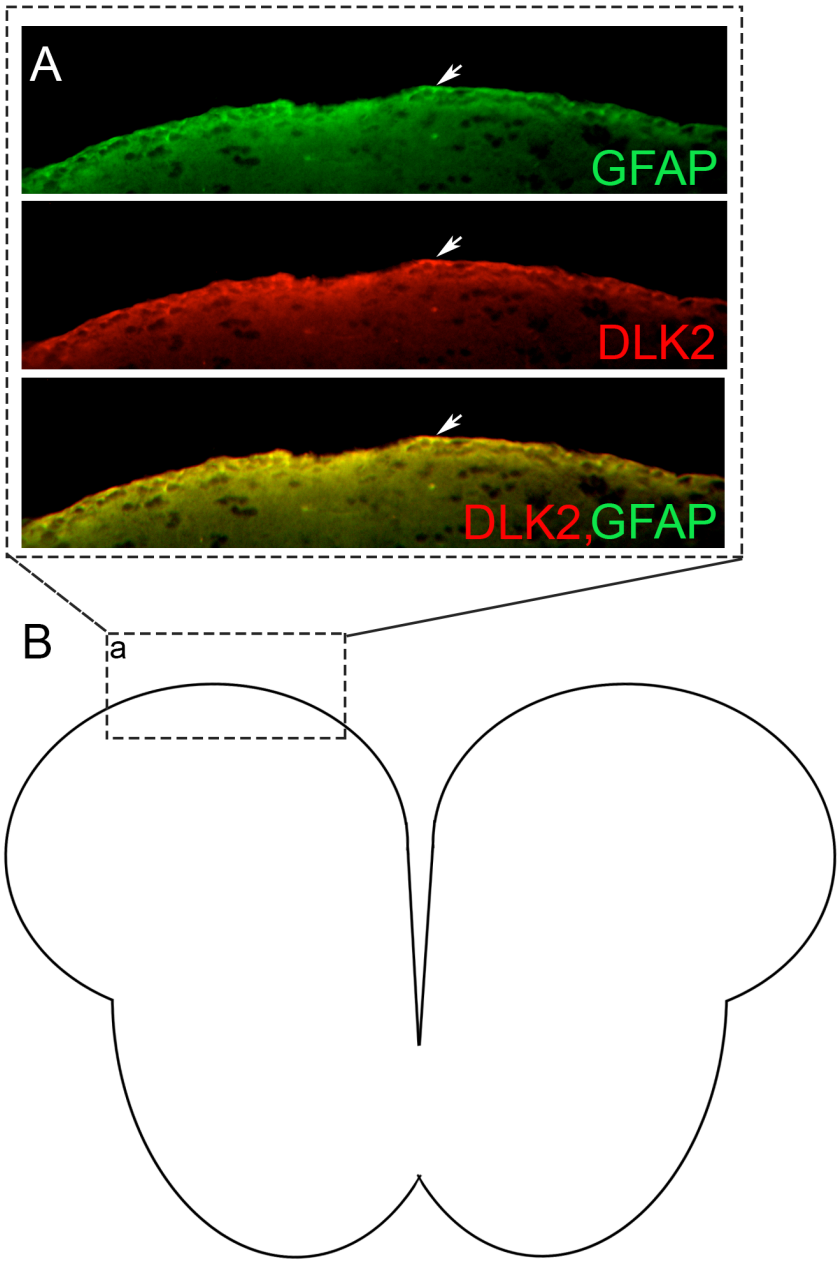

Figure 3.12 | DLK2 IHC shows that presence of DLK2 in radial glial cells. A., a representative image of the peripheral cell layer on a transverse section of adult telencephalon. IHC was performed with DLK2 antibody in the context of a gfap:gfp transgenic zebrafish to identify the radial glial cell population. DLK2 is co-localised with the gfp signal under the control of the gfap promoter, demonstrating the presence of the DLK2 protein in the radial glial cell population. **B.,** schematic representation of a transverse section through the adult zebrafish telencephalon with boxes demonstrating where the rest of the images in the figure are situated

3.3 Conclusion

The investigations described in this chapter have shown that both *dlk1* and *dlk2* are expressed during zebrafish embryonic development. Zebrafish *dlk1* and *dlk2* share very similar expression patterns, with subtle differences between the two. Namely, *dlk2* expression becomes restricted to the anterior of the embryo earlier in development than *dlk1* (Fig. 3.13). Furthermore, when *dlk1* and *dlk2* become highly localised in the zebrafish larval brain, their expression is in distinct regions from one another. This study identified two interesting areas in which to further examine the function of these genes: 1) The neural regions of the larval brain and 2) the radial glial cells in the adult telencephalon.

Dlk1 and *dlk2* have very different expression domains when compare to *Dlk1* in mouse. However, there are similarities in their expression when compared to *Dlk2* expression in mouse embryos (Fig 3.14; data provided by Alex Ashcroft). Murine *Dlk2* has much broader expression than *Dlk1*, and it is also highly expressed in neuronal regions. Taken together, this suggests that neuronal expression of *dlk1* and *dlk2* may well be the ancestral state of the gene and the differences observed in *Dlk1* expression in mouse may be a result of the evolution of mammalian-specific functions.

Figure 3.13 | Summary of *dlk1* and *dlk2 in situ* throughout zebrafish embryonic development.

This figure shows a full comparison of *dlk1* and *dlk2 in situ* through development for the sack of ease of comparison between the two. The figure also shows some controls: Sense probe controls that were used to demonstrate the specific nature of the anti-sense probe signal, and *shh* probes that were used in order to demonstrate the effectiveness of the *in situ* method. This probe was selected because of its well characterised and discrete domain of expression and to demonstrate probe penetration due to the location of the signal in the centre of the larval zebrafish.

Shh
Anti-sense
Dlk2
Sense
Dlk1
Sense
Anti-sense
Stage
Bud (10 h.p.f.)
18 somite (18 h.p.f.)
Prim-6 (25 h.p.f.)
Prim-16 (31 h.p.f.)
High-pec (42 h.p.f.)
Long-pec (48 h.p.f.)
Pec-fin (60 h.p.f.)
Protruding mouth (72 h.p.f.)
Day 4 (96 h.p.f.)
Day 5 (120 h.p.f.)

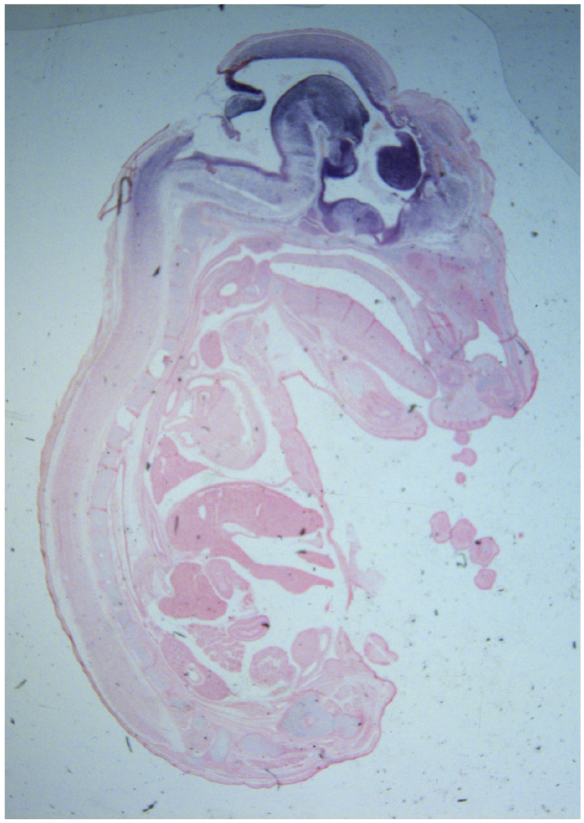

Figure 3.14 | *Dlk2* is expressed throughout the E16.5 mouse embryo brain. Preliminary studies into *dlk2* expression in mouse (Performed by Alex Ashcroft) show that *dlk2* is expressed throughout the E16.5 mouse brain. Little expression is seen in other tissues.

4. Approaches to knock-down and knock-out *dlk1* and *dlk2* in zebrafish

4.1 Introduction

The aim of this thesis is to understand the mechanisms by which *dlk1* and *dlk2* function. The first approach to examine this was to use available knock-down approaches. Murine *Dlk1* has been demonstrated to be highly dosage dependent (Charalambous et al., 2012). This supports the approach of examining the effects of *dlk1* and *dlk2* knock-down. However, murine *Dlk1* behaves in an autocrine, paracrine and endocrine manner (Cleaton et al., 2016; Ferrón et al., 2011; Sul, 2009). When multiple different forms of action are operating simultaneously, an extra level of complexity is added when it comes to interpreting knock-down phenotypes and elucidating mechanistic function. Therefore, producing a genetic mutant was a key aim of this project. The targeted genomic knockout technology CRISPR-Cas9 was described during the course of this project (Le Cong et al., 2013). Experiments were performed to optimize this technology and to produce *dlk1* and *dlk2* mutants using this system, but the generation of *dlk1* and *dlk2* targeted mutations was not successful.

Morpholino oligonucleotides (MOs) are anti-sense oligonucleotides that target the gene of interest and are specifically designed to the ATG start site to block translation, or to intron/exon splice boundaries to block the correct splicing of the target RNA (SUMMERTON and WELLER, 1997). They have been frequently used in zebrafish as a mechanism for targeted gene knock-down. However, analysis of morpholino knock-down phenotypes that have been previously described show very little correlation to phenotypes that result from genomic mutations of the same gene (Kok et al., 2015). Another study determined that the differences between the morpholino knock-down and a genomic mutation phenotype can be due to genetic compensation mechanisms (Rossi et al., 2015). Ultimately, MOs are a useful knock-down approach, but it is clear that there are numerous off-target effects (Rossi et al., 2015). In order to mitigate off-target effects, a mismatch MO is used, demonstrating that the MO with a 4bp mismatch from the target has no phenotype, which provides some evidence against off-target effects (PARTRIDGE et al., 2009). However, it

is still not possible to mitigate against all off-target effects and this will always cause difficulty in interpretation of MO results.

This chapter describes the results of MO studies targeting *dlk1* and *dlk2*. However, mismatch controls designed as variants on the *dlk1* MOs were always found to produce abnormal phenotypes. Mismatch controls for *dlk2* MO injections yielded clean results, free from any abnormalities, and so only results of *dlk2* knock-down are presented here.

4.2 Results

4.2.1 MO knockdown of *dlk2* leads to developmental abnormalities.

To investigate the role of *dlk1* and *dlk2* in early zebrafish development, translation-blocking MOs were used to transiently knockdown expression of *dlk1* and *dlk2*. In the initial analysis of the MOs, both a 25bp anti-sense oligonucleotide targeting the translational start site and a 5bp mismatch (MM) control were used to determine the specificity of targeting MOs. Several MO/MM pairs were tested for *dlk1*, but as both the MO and the MM displayed the same phenotypes in all cases, these were not analysed further. A concentration analysis was performed on the *dlk2* MO and MM pair. This analysis was performed to determine the concentration at which no phenotype was seen in the MM control, as well as to observe the MO knockdown phenotype at different doses. Ultimately, the MO analysis revealed minor developmental abnormalities to the surface of the neuroepithelium that were identifiable on a dissecting microscope, which could be categorized as either having or not having "head defects" as compared to controls (Fig 4.1A and B). Injection of 0.05ng of MM showed very little developmental abnormalities, hence the rest of the experiments in this report were performed at the 0.05 ng concentration (Fig. 4.1B). To understand how the *dlk2* knockdown leads to the observed phenotypes, the earliest time point at which the defects manifest was determined. Another phenotype observed after MO injection was the reduction in

size of the developing zebrafish embryo. BrdU labelling was performed at 24 h.p.f. and 48 h.p.f. on the MO, MM and uninjected embryos. BrdU analysis revealed that proliferation rates are equivalent at 24 h.p.f.; however, the *dlk2* MO-injected embryos have massively reduced levels of proliferation at 48 h.p.f. (Fig. 4.1C).

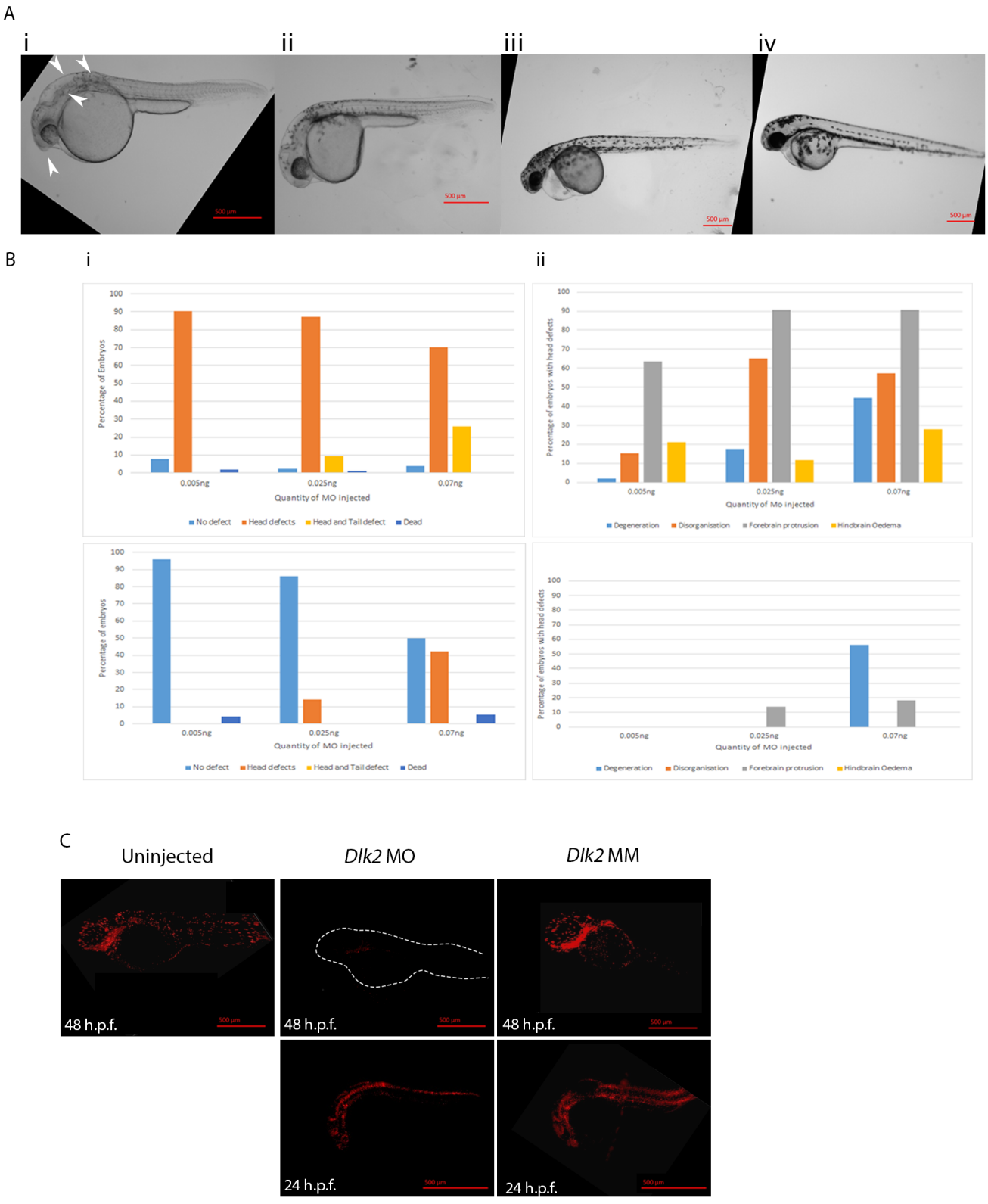

Figure 4.1| MO injection phenotypes of *dlk2* A. i. 0.025 ng injection of *dlk2* MO imaged at 24 h.p.f. when scored. Representative image with arrows pointing to the forebrain protrusion, perturbation of the hindbrain neuroepithlia, hindbrain odema and loss of pigmentation in melanocytes. ii. 0.025 ng injection of *dlk2* mismatch control displays no phenotype. iii 0.025ng injection of *dlk2* MO at 48 h.p.f. shows reduced head and body size. iv 0.025ng injection of *dlk2* mismatch control shows no phenotype at 48 h.p.f. B. Dosage analysis of *dlk2* MO and MM scored at 24 h.p.f. i *Dlk2* MO injected embryos. ii Mismatch control injected embryos. C. Representative image of BrdU incorporation in embryos injected with *dlk2* MO and mismatch at 48 h.p.f ad 24 h.p.f. Massive reduction in BrdU incorporation at 48 h.p.f, but not at 24 h.p.f.

4.2.2 Knockdown of *dlk2* leads to the reduction of a specific domain of Notch pathway activation.

To understand the effect of *dlk2* knockdown on the Notch signaling pathway, transgenic zebrafish containing eGFP driven downstream of a series of RBP-JK enhancer sites were used (Parsons et al., 2009). When the Notch signaling pathway is activated, the Notch intracellular domain (NICD) binds to its co-factors, including RBP-JK, and drives the expression of the eGFP. This provides a live readout of Notch activity. Analysis of embryos from the onset of expression of the Notch activation marker at 14 h.p.f. until 24 h.p.f. revealed no difference in Notch signaling activity in the *dlk2* MO-injected fish compared to the MM control. Between 24 h.p.f. and 48 h.p.f., however, there was a large amount of Notch activity in the hindbrain of the non-injected and MM-injected developing embryo, and this activity was markedly reduced in the *dlk2* MO injected embryos (Fig. 4.2). Figure 4.2 shows representative stills from a time lapse of development between 34 h.p.f. and 46 h.p.f. of development. In uninjected controls, there is a strong domain of Notch activation in the hindbrain during this period of development (Fig 4.2), which does not happen in the MO injected embryos (Fig 4.2). During this time, Notch is also active in the olfactory bulb, heart, trunk and tail. Notch activity in these areas was largely unperturbed in the *dlk2* MO injected fish, with defects restricted specifically to the hindbrain, which is an observation in keeping with the gross morphological defects observed (Fig. 4.2). This suggests that *dlk2* is involved in a very specific domain of Notch signaling during early zebrafish development.

A

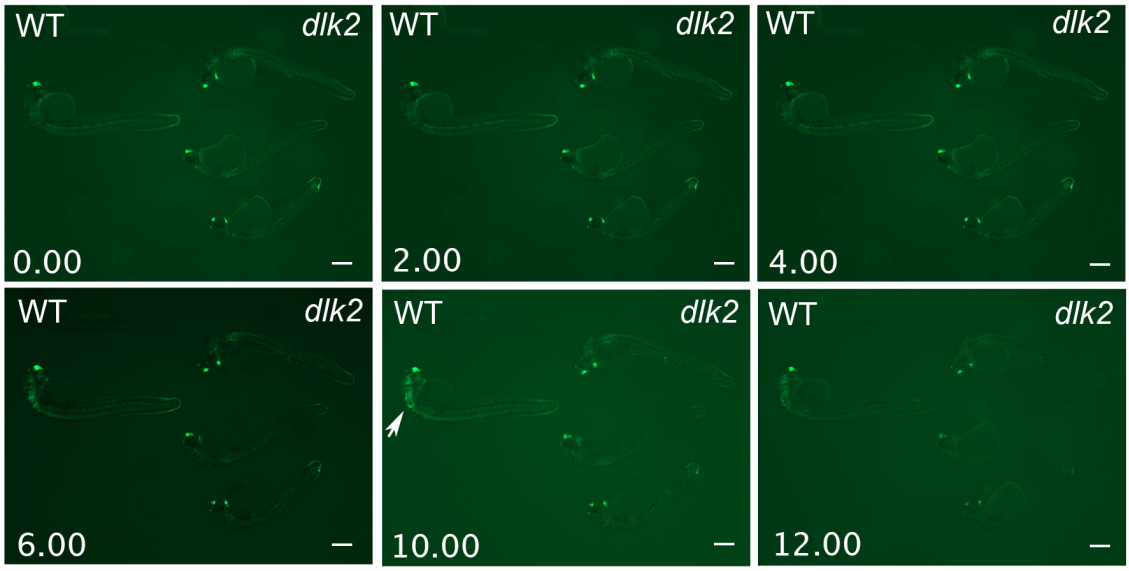

B

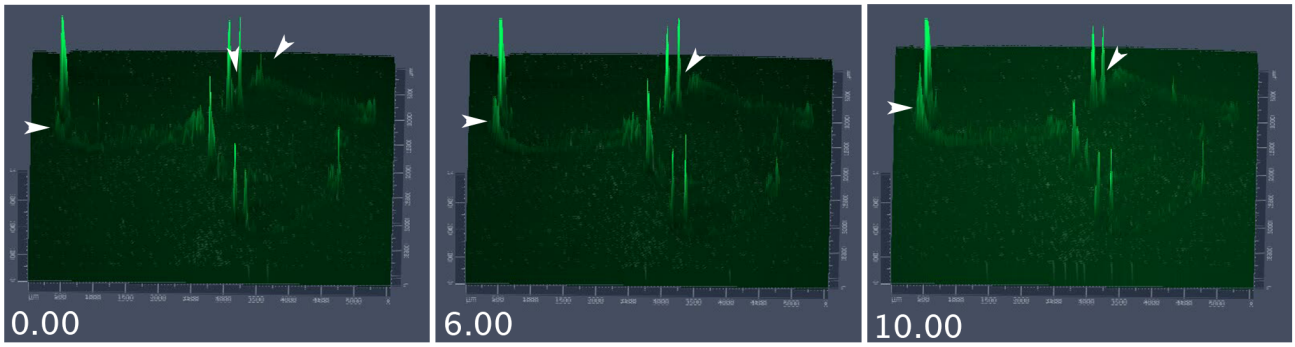

Figure 4.2| Timelapse of *dlk2* MO injected embryos with a fluorescent Notch reporter. A Stills from a 12 hour timlapse film from 34 h.p.f. to 46 h.p.f. On the left is a *dlk2* mismatch injected embryo and on the right three *dlk2* MO injected embryos with different severity of phenotypes. B Quantification of Notch reporter intensity shows an increase in signal in the hindbrain of the mismatch control, but not the MO injected embryos, highlighted with arrows. Notch reporter signal is still present in other areas of the *dlk2* MO injected embryos.

4.2.3 *Dlk2* MO knockdown leads to a reduction in Dlk2 protein.

Zebrafish embryos were injected with 0.025ng of the *dlk2* MM control and MO and fixed at 24 h.p.f. IHC was performed using the Dlk2 antibody. In the MM control embryo, the Dlk2 antibody produced normal signal from the Dlk2 IHC (Fig. 4.3A). In the *dlk2* MO injected zebrafish, there was a reduced Dlk2 signal, demonstrating that *dlk2* MO injection leads to a reduction in Dlk2 protein levels.

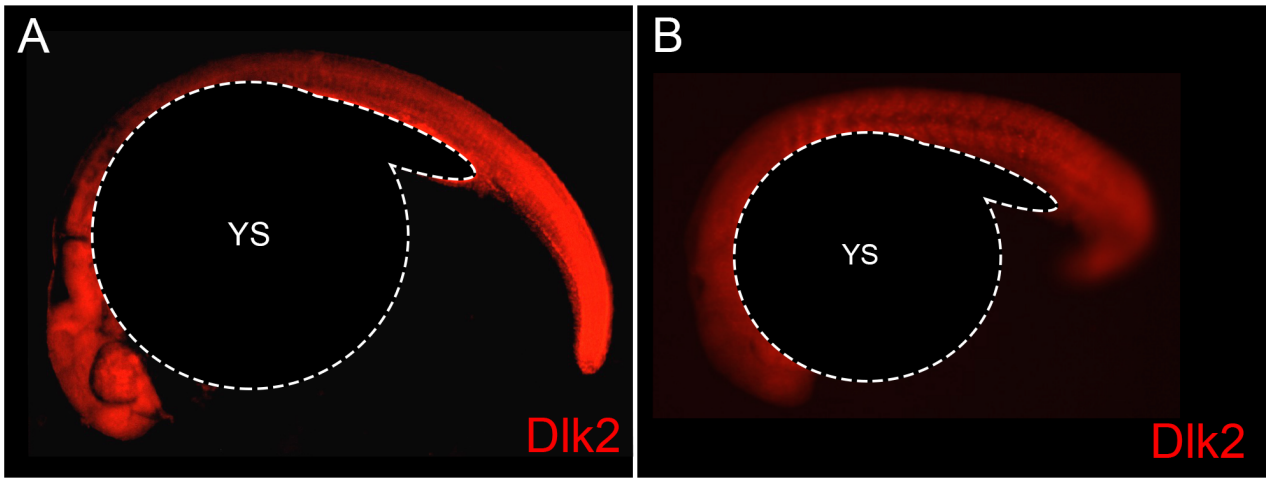

Figure 4.3 | There are reduced levels of Dlk2 protein in *dlk2* MO injected zebrafish. A. Shows a 24 h.p.f. zebrafish embryo that was injected with 0.025ng of *dlk2* MM as a control. There are normal levels and patterns of Dlk2 IHC localisation in the MM injected control. B Shows a 24 h.p.f. zebrafish embryo that was injected with 0.025ng of *dlk2* MO. There is a reduction in the Dlk2 IHC signal.

4.2.4 Using CRISPR-Cas9 to generate *dlk1* and *dlk2* mutants.

CRISPR-Cas9 mediated genomic editing was performed in zebrafish by co-injecting Cas9 RNA with the RNA of the guide for the target sequence. Injection conditions, guide RNA and Cas9 concentrations were optimised using guide RNAs designed to the albino locus (guide RNA plasmid kindly provided by Steve Harvey, Sanger Centre). Guide RNAs to zebrafish *dlk1* and *dlk2* were designed to Zv9 (genome release 9). Injections were performed at the previously optimised concentrations into eggs from wild type zebrafish lines and the Notch-reporter line. Several hundred embryos were grown from three separate rounds of guide RNA injection. These fish were grown on the system while a genotyping technique was developed. If the mutation occurred, the injected fish would be mosaic for the mutation, so instead of genotyping these fish directly, the fish were bred individually with wild type fish and the embryos produced were genotyped in pools. In any pools with positive genotyping results, the remaining embryos in the clutch were reared. These fish were then fin clipped and sequenced to find the nature of the mutation. Ultimately, the genotyping method produced false positives and none of the F2 zebrafish examined had a mutation in *dlk1* or *dlk2*.

Genotyping methods

When the experiment was started, it was the first of its kind to be performed in our facility and very early in the development of the CRISPR-Cas9 system. As such, there were no published genotyping methods for screening the mutations produced by the CRISPR-Cas9 system, only methodological studies. The first approach used was to amplify a 200bp PCR region spanning the CRISPR target site, with a restriction enzyme site within the guide sequence. A mutation occurring in the restriction enzyme site would cause failure of the PCR product to digest. Therefore, if any undigested PCR product remained, it would indicate that there is a mutation in the genomic DNA

within the target region. This approach did not identify mutations, and was assumed that it was because the restriction enzyme site might not always be the location of the mutation, which can occur around the guide site. The second genotyping method developed was a T7 endonuclease based approach. This approach had been described to work in identifying CRISPR mutations in *Drosophila* (unpublished; http://www.crisprflydesign.org/t7-endo-i-assay/). T7 endonuclease cleaves imperfectly hybridised DNA. After PCR of the region, T7 endonuclease is added to the reaction and any digestion is taken as an indication of a mutation. This technique proved inconsistent, often producing cleaved bands in wild type samples. The final genotyping method was using a high-resolution melting analysis. This technique had previously been described for use in identifying zebrafish mutations (Parant et al., 2009). Using this technique produced positive results. However, the genomic target regions of all fish with positive results from high resolution melting analysis were sequenced and these were ultimately found to be false positives and did not produce a mutant.

4.3 Discussion

MOs are the knockdown technology of choice and when appropriate controls are used they can yield useful results to examine the consequences of gene knock-down (Eisen and Smith, 2008). In addition to the appropriate controls, the gold-standard method of validating the MO phenotype is to rescue it by injection of the mRNA of the knocked-down gene. However, ubiquitously overexpressing the target gene by mRNA injection can lead to its own set of defects. This experiment was not preformed as there was concern over dosage effect, given that dosage is critical in the mouse system (Charalambous et al., 2012). Also, efforts were redirected towards making stable genomic mutations on the assumption that this would validate the defects observed with the MO. Off target effects are frequently seen in brain development, such as degeneration in the brain leading to 'cloudy heads', making interpretation of knockdown effects of genes expressed in

neuronal development particularly tricky. Due to these difficulties, it was determined that, in the case of determining the function of *dlk1* and *dlk2*, it was not scientifically justified to develop this approach further. Therefore, the MO data shown here is somewhat preliminary. However, the later developed DLK2 antibody demonstrated a reduction in DLK2 protein levels. This strengthens the inclusion of MO data in this thesis to further our understanding of *dlk2* function.

The novel knockout technology, CRISPR, was only first reported in early 2013 at the start of this project, with no existing experience of using this technology within the lab (Le Cong et al., 2013). Experiments were performed using guide RNAs targeting the Albino locus that demonstrated successful knock-out by pigmentation loss. However, no *dlk1* or *dlk2* mutants were identified during the course of this project. One limitation of the CRISPR technology in targeting *dlk1* and *dlk2* is that the genomic sequence of these genes contains very few PAM domain sequences which are a necessary part of the guide RNA sequence design. In particular, the section of *dlk2* that was targeted was highly GC rich, which leads to difficulties in genotyping and PCR errors caused by this are very likely to be a source of false positives in genotyping.

4.4 Conclusion

The production of a *dlk1* and *dlk2* mutant through CRISPR-Cas9 mediated genome editing was not possible in the time span of this thesis. At the point that the genotyping method was successfully and consistently in place, and the false positive mutants had been successfully ruled out, there was no longer time in the project to generate a new mutation. While zebrafish have rapid embryogenesis, the generation time (time to maturity) is still 3 months. This means that generating a stable mutation can take upwards of a year and, depending on the level of backcrossing determined to be necessary in order to remove off-target mutations, can take even longer. Transcription activator-like effector nucleases (TALENs) were not used in this project because, at the time, it was considered to be the inferior genome editing technology. This was largely because of the increased time in producing the specific targeting plasmid and what was then believed to be

less efficient genome editing rates. If *dlk1* and *dlk2* mutant zebrafish are to be attempted again in the future, TALENs could be a better option because they would be less limited in where they can target within these genes. It is also becoming increasingly clear that different guide RNAs and different genes have vastly different efficiencies of mutation and off-target effects with CRISPR technology (Wu et al., 2014). Unpublished data within the lab shows that targeting *Dlk2* with CRISPR in mouse has been similarly unsuccessful so far, while other genes targeted with the identical technique have had very high levels of success (pers. comm. Anne Ferguson-Smith). However, efficiency of CRISPR-Cas9 mediated genome editing is constantly progressing and it may well be worth attempting it again in the future (Burger et al., 2016).

The MO study demonstrated that Dlk2 protein was reduced, and even with the difficulty of off-target effects, this could still be a useful tool for examining *dlk2* function in the future. One possibility is to use splice-site blocking MOs instead of the translation blocking ones used in this study, as they allow direct validation of knockdown through analysis of the mRNA. The second possibility is to use the photo-cleavable MO for a targeted knockdown in specific locations (Sumanas, 2017; Tallafuss et al., 2012).

5. Analysis of *dlk2* mutant zebrafish.

5.1 Introduction

To understand the function of the ancestral *dlk2* gene, examination of a mutant zebrafish was essential. Unfortunately, the efforts to produce a mutant during this project were unsuccessful, as described in Chapter 4. However, during the course of this project, a *dlk2* mutant became available from the Zebrafish Mutation Project. The mutation occurs in an essential splice site at the beginning of exon 4 (Fig. 5.1). Exon 4 contains multiple EGF repeats and exon 5 contains the trans-membrane domain. Aberrant splicing at the start of exon 4 is predicted to result in a nonsense transcript and premature truncation of this gene before exon 4. This is predicted to result in a null mutation, as the EGF repeats and transmembrane domain are thought to be essential for Dlk2 function (Fig. 5.1).

The purpose of this study was to examine the *dlk2* mutant zebrafish to understand the function of this gene in zebrafish development, as well as to provide model systems that can be examined to understand the mechanism by which this gene operates. This chapter describes the characterisation of the *dlk2* mutant zebrafish, with the aim of identifying aberrant developmental features that demonstrate the functional role of *dlk2* and to provide a system in which to examine its function.

5.2 Results

5.2.1 *dlk2* mutant from the Zebrafish Mutation Project has no detectable DLK2 protein using IHC with the DLK2 antibody.

A DLK2 polyclonal antibody was generated in collaboration with Abcam, using the whole recombinant human DLK2 protein as the antigen. The antibody did not detect a band at the predicted molecular weight of zebrafish Dlk2 (42 kDa); however, whole mount IHC was

performed and produced a specific signal in the same locations as the *dlk2* ISH (see section 3.**x**). Whole mount IHC was performed on wild type and *dlk2* mutant zebrafish embryos (Fig. 5.2). At 24 h.p.f., there was no signal at all from the Dlk2 IHC (Fig. 5.2B). At 5 d.p.f., there is a small amount of signal produced by the Dlk2 IHC in the *dlk2* mutant (Fig. 5.2C). This signal is largely constrained to external surfaces, suggesting it is non-specific. However, there may be some weak cross-reactivity with similar proteins, such as Dlk1. This result supports the prediction that there is no Dlk2 protein produced in the *dlk2* mutant zebrafish.

5.2.2 No gross morphological defects are observed in the embryonic development of *dlk2* mutants.

Morphological analysis was performed on the embryos of the developing *dlk2* mutants using a developmental checklist to identify possible defects. Murine *Dlk1* mutants suffer from growth retardation, but no growth defects were found in the zebrafish mutants. No obvious defects were found in the morphology of the developing zebrafish (data not shown).

5.2.3 *dlk2* mutant larvae show a reduction in Notch signalling and an increase in the levels of GFAP protein

The *dlk2* mutation was bred into the Notch responsive zebrafish model. This transgenic zebrafish has a series of RBP-jk sites driving a fluorescent protein. These enhancer sites are bound by the Notch intracellular domain and its co-factors, so the fluorescent protein will be expressed wherever Notch signalling is active (Parsons et al., 2009). These Notch-responsive *dlk2* mutant embryos were examined. At 48 h.p.f. there is a reduction in Notch active signal in the embryonic brain (Fig. 5.3), consistent with the result observed with *dlk2* morpholinos (Section 4.2). Whole

mount IHC was performed on the *dlk2* mutant zebrafish using the GFAP antibody. At 48 h.p.f., there is a striking increase in GFAP protein in *dlk2* mutant embryos (Fig 5.4).

5.2.4 GFAP protein is depleted in larval stage *dlk2* mutants.

IHC was performed on hatching stage (72 h.p.f.) embryos and early larval stage (5 d.p.f.) zebrafish. The numbers of GFAP positive cells were reduced in the *dlk2* mutant hatching embryos and almost completely absent in the larval zebrafish (Fig 5.5).

5.2.5. Cell proliferation analysis

In order to determine if the increase of GFAP protein was due to an increase in proliferation of cells that have high GFAP levels, or if the high levels of GFAP were independent of an increase in cell numbers, a BrdU analysis was performed (Materials and methods, 2.6). BrdU is incorporated into the DNA of cells that divide during the period of BrdU exposure (pulse period). This becomes diluted by further cell divisions after BrdU washout (chase period). Therefore, experiments were performed with collection and fixation of embryos immediately after BrdU washout. There were much higher levels of BrdU signal in the 48 h.p.f. *dlk2* mutant zebrafish (Fig 5.6E), and the BrdU was highly co-localised with the GFAP IHC signal (Fig. 5.6). This demonstrates that the neural progenitor cells have increased levels of proliferation at early stages and this cell population is subsequently depleted by the early larval stage.

5.2.6. Behavioural analysis of larval zebrafish demonstrates that *dlk2* mutant larvae have increased motility.

To examine the behavioural consequences of the over-proliferation and subsequent depletion of the neural progenitor cell population, tracking of the larval zebrafish was performed using multi-well plate tracking apparatus. Initial examination (n=24) of *dlk2* mutant larvae movement suggests that they have increased locomotion activity (Fig. 5.7). A significant difference was found between the genotypes ($F(1,132)=4.86$, $p=.029$; ANOVA). *Dlk2* mutant zebrafish fish ($M=4294.57$px ±960.26) travelled significantly more distance overall compared to control fish ($M=2178.29$ px ±960.26). No significant time period ((MOVEM) ($F(5,132)=.41$, $p=.842$)), nor a time period x genotype interaction, ($F(5,132)=.955$, $p=.448$) was seen.

5.2.7. Radial glia are absent in the telencephalon of adult *dlk2* mutants.

The radial glial cells in the adult telencephalon were identified as expressing *dlk1* and co-localising with Dlk2 protein (Section 1.4). Therefore, radial glial cells were examined in the *dlk2* mutant zebrafish to determine whether *dlk2* was involved in their regulation. IHC was performed using the GFAP antibody, and found that in the *dlk2* mutants, there were no GFAP positive cells in the periventricular zone (Fig 5.8). This demonstrates that the radial glial cell population is absent in the adult *dlk2* mutant zebrafish telencephalon.

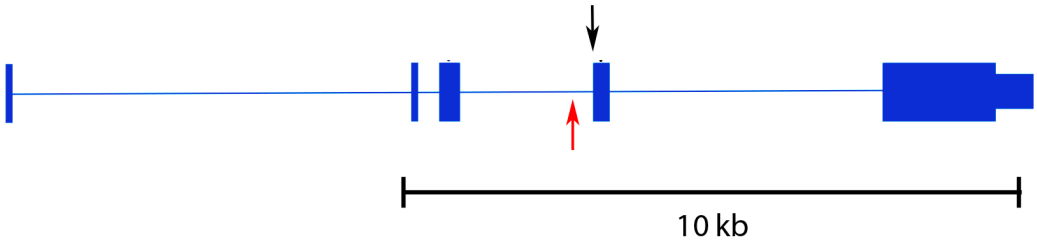

Figure 5.1 | *Dlk2* mutation produced by zebrafish mutation project. This figure shows the exon and intron structure of *dlk2*. The black arrow points to the site of the mutation. The red arrow points to a stop codon in the intronic sequence that will be maintained. The vast majority of the coding sequence for *dlk2* is after the predicted stop codon.

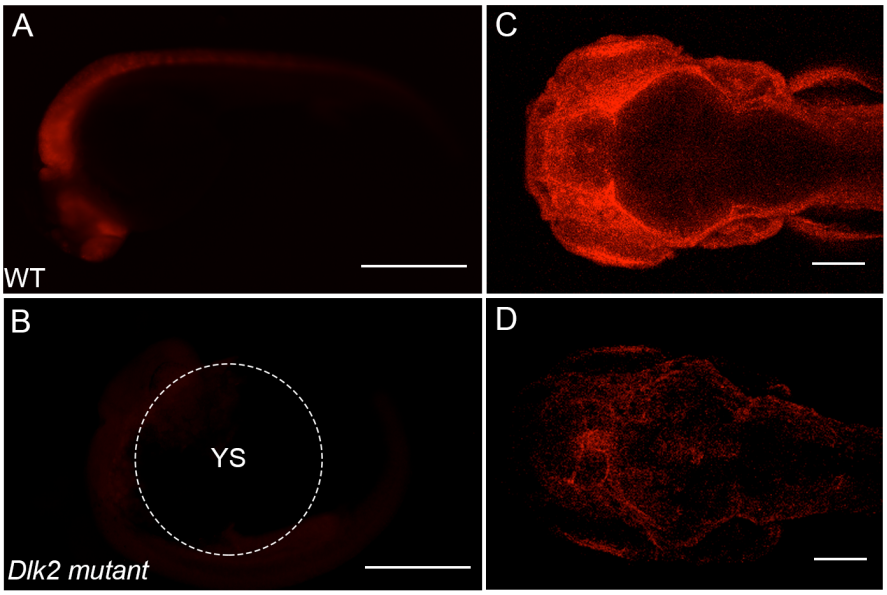

Figure 5.2 | No detectable Dlk2 protein in the *dlk2* mutant zebrafish. A Dlk2 IHC in 24 h.p.f. zebrafish embryo, shows expected Dlk2 signal. B No Dlk2 IHC signal in the 24 h.p.f. mutant zebrafish embryo. C A Dlk2 IHC in 5 d.p.f. zebrafish embryo, shows expected Dlk2 signal. D Only low backgorund levels of Dlk2 IHC Signal in *dlk2* mutant embryo. Scale bar, 0.5mm.

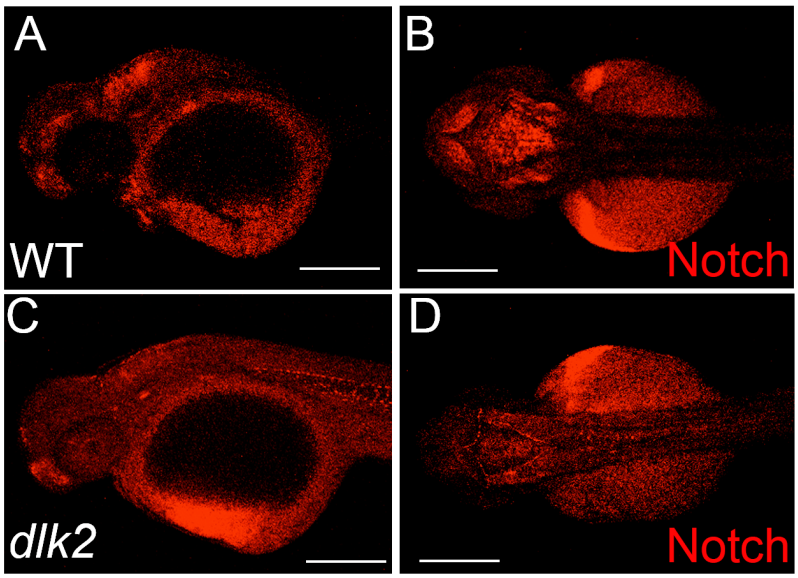

Figure 5.3 | *Dlk2* mutation leads to reduced Notch activation at 48 h.p.f. A 48 h.p.f. wild type Notch-resposive transgenic zebrafish. There is clear Notch activation in the hindbrain. B Dorsal view of a 48 h.p.f. wild type Notch-resposive transgenic zebrafish, with clear hindbrain Notch responsive siganling. C and D The lateral and dorsal view, respectively of the *dlk2* mutant Notch-responsive transgenic zebrafish. There is a reduction of Notch activation in the embryo, in particular the hindbrain has lost most of its notch activation signal. Scale bar, 0.5 mm

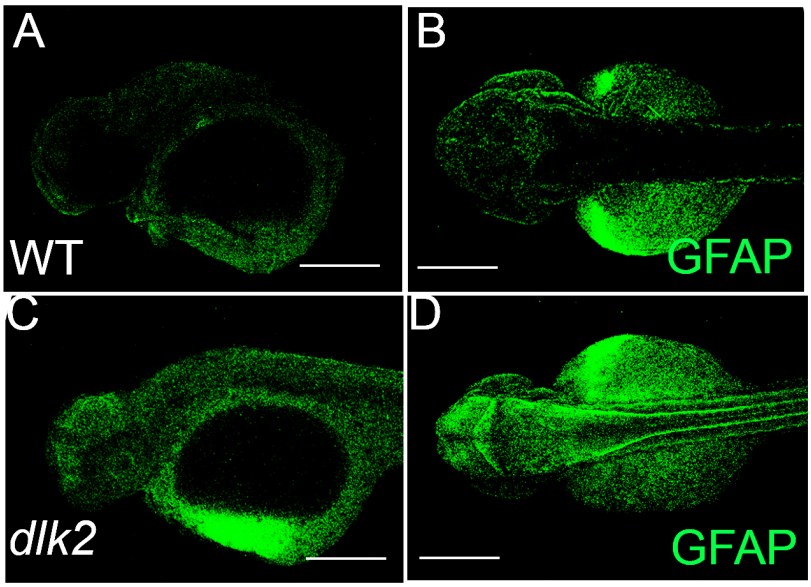

Figure 5.4 | *Dlk2* mutation leads to an increase in GFAP positive cells at 48 h.p.f. A and B a lateral and dorsal view, respectively, of GFAP IHC on a 48 h.p.f. wild type zebrafish. The GFAP antibody produces little signal at this stage in the wild type.. C and D The lateral and dorsal view, respectively of GFAP IHC on a 48 h.p.f. *dlk2* mutant zebrafish. There is an increase in the number of GFAP positive cells present in the *dlk2* mutant compared to the wild type. Scale bar, 0.5 mm

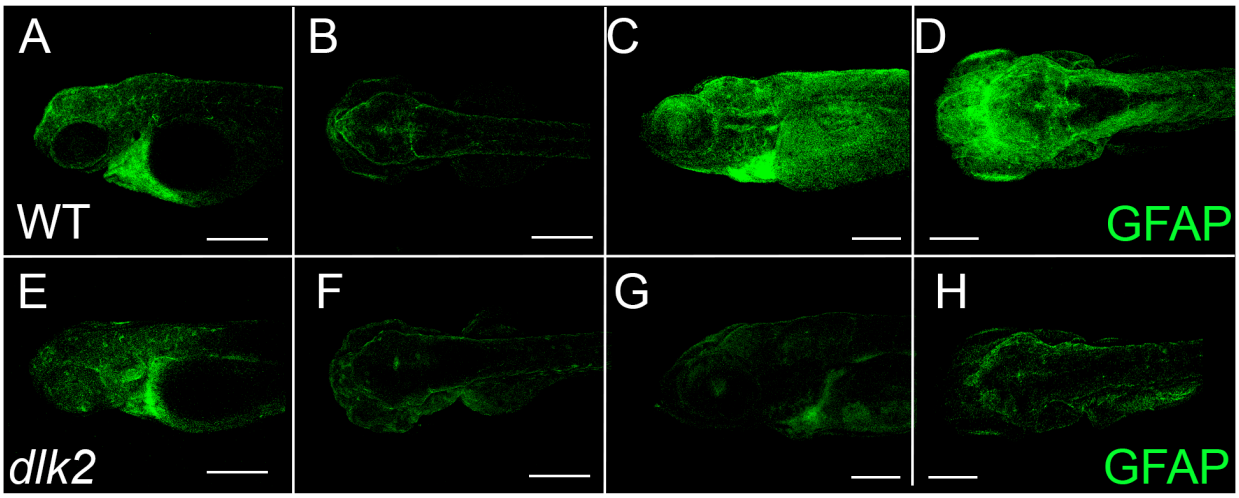

Figure 5.5 | The hatching and larval *dlk2* mutant zebrafish have a reduction in GFAP positive cells. A and B show the lateral and dorsal view of GFAP IHC in the hatching zebrafish embryo. GFAP positive cells can be seen to be appearing throughout the brain at this stage. E and F show the lateral and dorsal view of GFAP IHC in the *dlk2* mutant hatching embryo. There is a reduction in the amount of GFAP positive cells when compared to the wild type. C and D show the lateral and dorsal view of GFAP IHC in the larval zebrafish embryo. There is a high number of GFAP positive cells throughout the larval brain. G and H show the lateral and dorsal view of GFAP IHC in the larval *dlk2* mutant zebrafish embryo. There is a almost complete depletion of GFAP positive cells as compared tot the wild type. Scale bar, 0.5mm

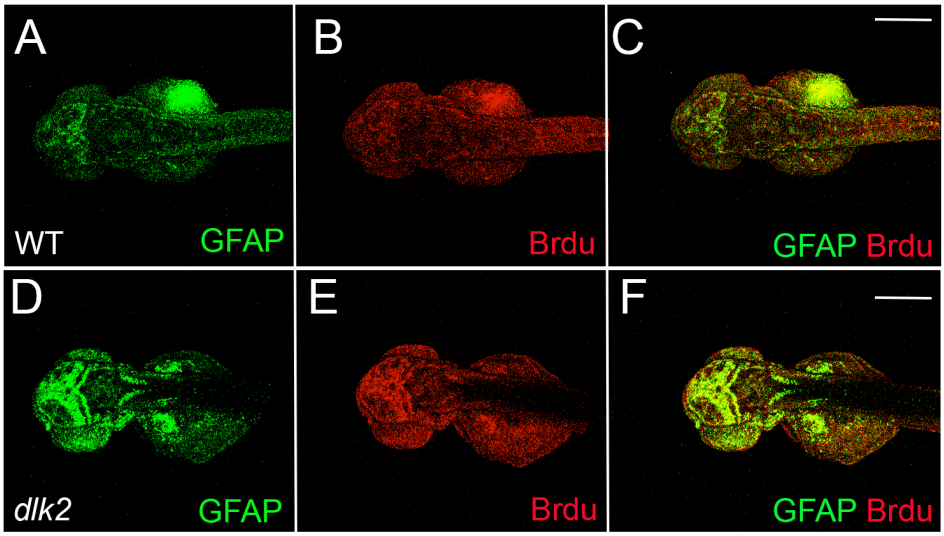

Figure 5.6 | The *dlk2* mutants have increased proliferation in the additonal GFAP positive cells. A, B and C show a wild type 48 h.p.f. zebrafish that has been exposed to Brdu for 5 minutes before fixation. GFAP IHC was performed to examine the co-localisation of the proliferation, Brdu signal, and presence of GFAP. A shows there is low levels of GFAP positive cells. B shows low levels of Brdu signal. C shows a merged image of the GFAP and Brdu, showing somewhat of an overlap between the two. D, E and F show a *dlk2* mutant 48 h.p.f. zebrafish that has been exposed to Brdu for 5 minutes before fixation. GFAP IHC was performed to examine the co-localisation of the proliferation, Brdu signal, and presence of GFAP. A shows the expected high levels levels of GFAP positive cells. B shows a high level of Brdu signal. C shows a merged image of the GFAP and Brdu, showing an overlap of signal between the two. This demonstrates that the GFAP positive cells are highly proliferative in the *dlk2* mutant embryo. Scale bar, 0.5mm

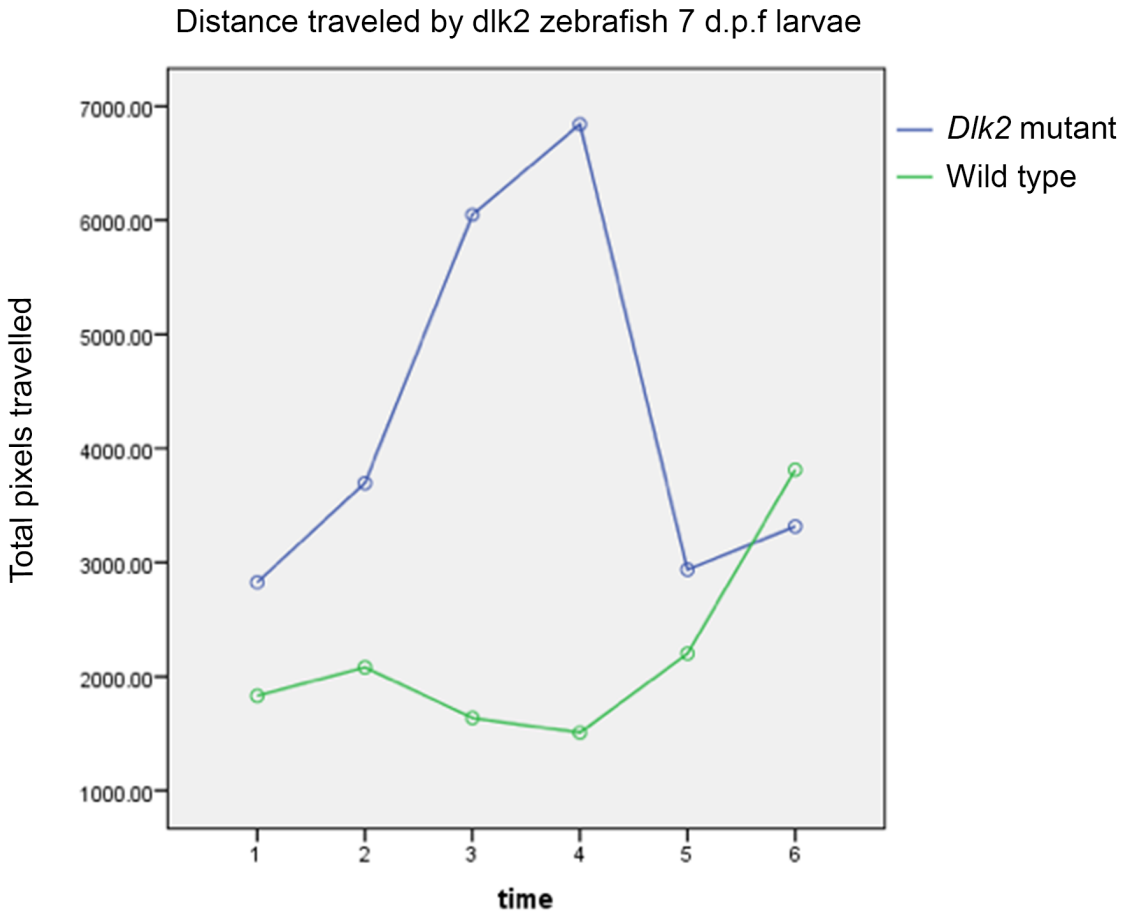

Figure 5.7 | *dlk2* mutants have increased levels of locomotion at 7 d.p.f. The graph shows the number of pixels (arbitrary measurement of distance) moved on average by the *dlk2* mutant and wild type zebrafish over 6 different 5 minute time periods. The graph shows that *dlk2* mutant zebrafish moved move over this time period than the wild type.

Figure 5.8 | The radial glial cell population is not present in adult *dlk2* mutant zebrafish.

A section from a wild type adult zebrafish telencephalon with GFAP IHC performed on it. The GFAP IHC show clear radial glial cell populations, as shown by arrows. **B** section from a *dlk2* mutant adult zebrafish telencephalon with GFAP IHC performed on it. The GFAP positive radial glial cells are not present. C A schematic diagram of the adult telencephalon section, with a diagram representing where the images A and B are located.

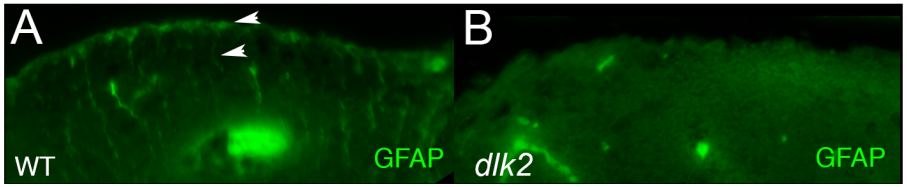
A
WT
GFAP
B
dlk2
GFAP

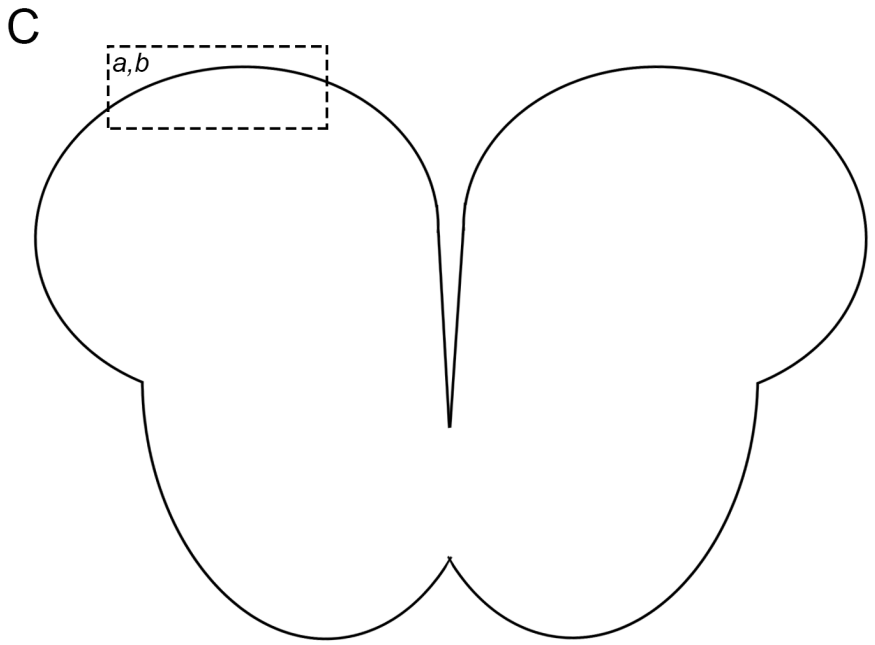
C
a,b

5.3 Discussion

The aim of this chapter was to elucidate the function of *dlk2* by examining the consequence of *dlk2* mutation on the development of zebrafish embryos. The lack of signal observed following IHC with the Dlk2 antibody (Section 5.2.1) supports the prediction that the mutation produced by the Zebrafish Mutation Project results in a complete loss of Dlk2 protein. In wild type zebrafish, *dlk2* was found to be highly expressed throughout the zebrafish brain using ISH analysis performed in Chapter 3, as well as in endodermally- and mesodermally-derived tissues. Therefore, it was predicted that the loss of *dlk2* would lead to morphological and developmental abnormalities. Morphological examination of the *dlk2* mutant embryos revealed that the embryos develop normally. No gross morphological abnormalities were detected. It is currently unknown what the effect of *Dlk2* mutation would be in the mammalian system; however, *Dlk1* mutation leads to growth retardation and obesity in mice (Moon et al., 2002). The lack of developmental abnormalities in the zebrafish could be due to differences in biology between mice and zebrafish. The growth retardation phenotype could be caused by misregulation of hormones not present in zebrafish. In this case, an obesity phenotype would not be observed, as the first adipose deposition occurs after 5 d.p.f., which occurs outside the scope of this investigation (Flynn et al., 2009). An alternative explanation is that *dlk2* functions in zebrafish could be partially redundant; potentially, they could be compensated for by the activity of *dlk1,* which has a very similar expression pattern in early zebrafish embryogenesis. Another explanation is that there are differences in the functional roles of *dlk2* in zebrafish and *Dlk1* in mouse.

The neural progenitors were the focus of investigation for this study because of the strong *dlk2* expression present throughout the zebrafish embryonic brain and the known role of murine *Dlk1* in regulating NSCs (Ferrón et al., 2011). The co-localisation of BrdU signal and the increased GFAP protein levels supports the conclusion that the changes is GFAP levels are due to an

increase of cells with high GFAP protein levels. Further, the loss of Notch-activation signal can be hypothesised to be due to a reduction of cell numbers that express Notch signalling. From this, it was concluded that an initial loss of Notch-activated cells was observed with a concurrent expansion of the transit amplifying neural progenitor population through increased proliferation (Summary Fig 5.9). Later in development, the neural progenitor population is depleted. These results lead to the hypothesis that the premature and over-differentiation of the NSC population leads to a large increase in GFAP positive cells that terminally differentiate, most likely into primary motorneurons (Bingham et al., 2003). Later in development, there would be no NSCs left to produce the correct GFAP positive cell populations. However, it is possible that the changes in GFAP and Notch activity are due to cell autonomous expression changes rather than changes in cell numbers. This too could lead to changes in cell fate, which would account for the differences observed in the mutant.

The *dlk2* mutants also demonstrated increased levels of locomotion in a preliminary larval tracking study. This phenotype could be explained by increased specification of primary motorneurons, expected from the expansion of the early neural progenitor pool (Appel et al., 2001; Bingham et al., 2003). If this hypothesis is correct, it may lead to later neurological defects with a lack of the secondary motorneuron populations and glial cells, which are produced by the neural progenitors (Johnson et al., 2016). Further work examining the number of different cell types present and their population sizes could be performed to confirm this phenotype.

The final result presented in this chapter is the loss of radial glial cells in the adult telencephalon of the *dlk2* mutant. It is unknown if this is because of a later aberrant specification of the radial glial population, or if these cells are derived from the cell populations missing in the *dlk2* mutant. The radial glial cells in the adult telencephalon have been shown to be responsible for the regeneration occurring in response to injury of the telencephalon (Kroehne et al., 2011). It would be of great interest to examine the effect of a brain lesion assay in a system when the radial glial cells are missing, such as the *dlk2* mutant zebrafish. In particular, it would be interesting to

examine whether other cell populations are able to take over the role of the radial glial population or whether regeneration will be impossible. Upon injury to the brain, there is an initial inflammatory response. In mammals, the inflammatory response is maintained, which leads to an environment that is not conducive to regeneration and a glial scar is formed. Zebrafish, on the other hand, are able to suppress the inflammatory response, promote a neurogenic environment, and are able to fully regenerate the injury (Baumgart et al., 2012). It would be interesting to examine the role of the radial glial cells in dampening the inflammatory response and in creating the environment that allows them to repopulate the injured site.

5.4 Conclusion

The ultimate aim of this project was to describe a model system in which the mechanisms of *dlk2* function can be elucidated. The role of *dlk2* in the regulation of zebrafish embryonic neural progenitor populations is an ideal system. The results presented here suggest that *dlk2* is involved in the regulation of these neural progenitor populations. The high similarity of phenotype between *dlk2* mutation and aberrations in the Notch signalling pathway highly suggest that *dlk2* operates via the Notch signalling pathway in this developmental context. This has not previously been demonstrated in an *in vivo* system and hence provides a tool for further detailed investigations.

6. Discussion

6.1 Introduction

The purpose of this project was to establish a zebrafish model system to elucidate the mechanisms of *dlk1* and *dlk2* function. In order to achieve this, the aim was to answer the following questions:

1) **Where and when are *dlk1* and *dlk2* expressed during zebrafish development?**
    a. How does this compare to the known expression of *Dlk1* in murine development?
    b. Which cell populations expressing *dlk1* and/or *dlk2* could be used as model systems to examine their function?
    c. Where is *dlk1* and *dlk2* expression in relation to Notch signalling?
2) **What are the functional consequences of a *dlk2* mutation?**
    a. Are there any gross morphological phenotypes in *dlk2* mutant zebrafish embryos?
    b. How are the model systems which normally express *dlk2* affected by loss of its expression?
    c. How does the function of zebrafish *dlk2* compare to that of murine *Dlk1*?

In summary, the results presented in this thesis demonstrate that:

i) Both *dlk1* and *dlk2* are expressed during zebrafish embryonic development. There are some similarities between the embryonic expression of *dlk1* and *dlk2* in zebrafish with the expression of murine *Dlk1*.

ii) Zebrafish *dlk1* and *dlk2* are expressed in specific cell populations in the larval brain, which overlap with both Notch signalling and the GFAP positive radial glial cells responsible for generating neuronal populations.

iii) *Dlk1* is expressed in the radial glial cells of the adult telencephalon. The DLK2 antibody shows localisation of DLK2 protein in the radial glial cells. These cells are known to be regulated by Notch signalling.

iv) Loss of *dlk2* does not lead to any observed gross morphological phenotypes in the developing zebrafish embryo.

v) Loss of *dlk2* leads to early, rapid, cell division of the embryonic radial glial cells, causing a subsequent depletion of this cell population by 5 d.p.f. Preliminary evidence suggests this leads to behavioural abnormalities, which may be due to the incorrect specification of mature neuronal populations as a result of the disruption of the radial glial population.

vi) *Dlk2* mutants do not have the normal radial glial cell population in the adult telencephalon.

The differences between the expression of *dlk1* and *dlk2* in zebrafish and *Dlk1* in mouse may be due to differences in the functions of these genes between the two species. In particular, zebrafish *dlk1* and *dlk2* maintain high levels of expression throughout the developing brain, whereas mouse *Dlk1* becomes localised to just a few cell populations early in development. This may be due to evolutionary differences in the roles that *dlk1* and *dlk2* play in zebrafish development compared to the role of *Dlk1* in mouse. The more abundant expression pattern observed in zebrafish compared to mouse may represent an ancestral role of the genes or it may be representative of the difference in neurobiology between the two species. Zebrafish maintain much higher levels of neurogenesis throughout the developing embryo and in the adult brain (Paridaen and Huttner, 2014). The suggested role of *dlk1* and *dlk2* in regulating these neurogenic cell populations may explain the broader expression domain of *dlk1* and *dlk2* in the zebrafish brain.

The presence of *dlk1* and *dlk2* in both embryonic and adult radial glial populations, as well as the abnormal regulation of these populations in the *dlk2* mutant zebrafish, ultimately suggests that *dlk1* and *dlk2* are involved in the regulation of stem cell populations, as described in mouse. Therefore, this study demonstrates that zebrafish is an excellent model system to examine the mechanistic function of *dlk1* and *dlk2*, and it is likely that they operate through the same

mechanisms to regulate stem cell populations as observed in the murine system. Elucidating the mechanisms and signalling pathways that zebrafish *dlk1* and *dlk2* are operating through were beyond the scope of this study. However, the model system established produces a system that is available for further examination and will elucidate the mechanisms of *dlk2* function in zebrafish.

6.2 *dlk1* and *dlk2* expression in zebrafish and comparison to murine *Dlk1*

Comparing the embryonic development of mouse and zebrafish is inherently challenging. They are two very different organisms, with different life history traits, separated by hundreds of millions of years of evolution. Here it was demonstrated that *dlk1* and *dlk2* are expressed in zebrafish embryonic development, as *Dlk1* has previously been described in murine embryonic development. In addition, like murine *Dlk1,* zebrafish *dlk1* and *dlk2* are expressed in cells derived from all three germ layers (da Rocha et al., 2007; Yevtodiyenko and Schmidt, 2006). *Dlk1* in mouse is associated with numerous mammalian specific processes, being expressed in extra-embryonic tissues, and is also associated with the mammalian transition to independent life, including processes involved in thermoregulation (Charalambous et al., 2012; da Rocha et al., 2007). These structures and processes are fundamentally different and unique to mammals, hence there are no homologous tissues or physiological processes that could be examined in zebrafish. One of the most striking differences between mouse and zebrafish is the broad expression of *dlk1* and *dlk2* throughout the embryonic brain, whereas murine *Dlk1* is isolated to just a few locations in the embryonic brain (da Rocha et al., 2007). Murine *Dlk1* has been demonstrated to be a stem cell regulator (Section 1.4). In mouse embryogenesis, NSC pools get restricted to isolated zones, in particular to the ventricular zone and the subventricular zone (Zhang and Jiao, 2015). In zebrafish, on the other hand, the brain has many more sites of neurogenesis (Schmidt et al., 2013). Therefore, the broader expression of *dlk1* and *dlk2* throughout the embryonic brain may purely be representative of the additional levels of neurogenesis and NSC populations, rather than a

difference in function between these genes in mouse and zebrafish. However, preliminary studies of *Dlk2* expression in murine embryos show expression in post-mitotic neurons (pers. comm. Alex Ashcroft, Fig. 1.13). This is suggestive that there may be an additional function in the brain that could be ancestral and has been lost by murine *Dlk1* during the process of it being co-opted into mammalian specific processes.

Fundamentally, the aim of studying *dlk1* and *dlk2* expression in zebrafish development was to identify areas of expression and to use these areas of known expression for experimental study. It was shown that *dlk1* and *dlk2* are expressed in the region of neural progenitor populations and that the regulation of these cell populations is perturbed in *dlk2* mutants. This evidence suggests that *dlk2* is a stem cell regulator, just like *Dlk1* in mouse. It also suggests that the differences in expression in the brain are, at least in part, to do with the differences in neurobiology between the two organisms rather than a difference in function between the genes. Further study of murine *Dlk2* will help elucidate potential roles these genes might have in post-mitotic neurons. The zebrafish will remain an excellent model to further examine these functions (Section 6.5.1).

6.3 Function of *dlk2* in zebrafish

One of the aims of this study was to examine the role of *dlk2* in zebrafish development, with the ultimate aim of understanding the mechanisms by which *dlk2* operates. *Dlk2* represents the ancestral form of the *dlk1* and *dlk2* genes (Section 1.2). Therefore, understanding the mechanisms by which *dlk2* functions in zebrafish will give great insight into the functional mechanisms of this gene family as a whole and throughout the chordate phylum. This study morphologically described the *dlk2* mutant zebrafish and provided a model system in which to further examine the functional mechanisms of this gene. Combining the results of this project with existing literature has provided evidence for a model of *dlk2* mechanistic function in NSCs in the developing zebrafish brain, which is likely mediated through the Notch signalling pathway. These findings open up new

avenues for further research into regulation of neurogenesis and mechanisms of adult regeneration.

6.3.1 Morphological examination of *dlk2*

The mouse *Dlk1* mutation that has been described is a homozygous viable mutation (Moon et al., 2002). However, the *Dlk1*-null mouse does have gross morphological differences from that of wild type siblings. The most obvious differences are the increased fat deposition and growth retardation (Moon et al., 2002). Fat deposition in mouse embryos and neo-natal mice is much more apparent than in zebrafish. Post-natal mice must be able to regulate their own body heat and the fat reserves are extremely important for their thermogenesis (Rugh, 1968). Zebrafish, on the other hand, are thermoregulated by the temperature of the water they live in. The earliest signs of adipogenesis in the zebrafish are at 8 d.p.f., with fat droplets forming in the viscera (Flynn et al., 2009). The present study examined the embryonic development up to 5 d.p.f., so there may be adipogenesis defects occurring at time points that were not examined in this study. This could be an interesting future area of study (Section 6.6.3), as zebrafish is increasingly being considered as an adipogenic model with common pathophysiological pathways to mammals (Flynn et al., 2009; Oka et al., 2010). No apparent growth retardation was found in the *dlk2* mutant zebrafish. This could be because of the different roles of *dlk1* and *dlk2*, or perhaps due to the different physiology of the development of zebrafish relative to that of mouse. Another possibility is that the growth effects are impossible to identify because of the large variation in juvenile zebrafish size in normal conditions (Mabee et al., 2009). The variations in growth size can come from environmental factors such as density of animal stocking. However, they can also arise from the greater genetic background effects as zebrafish lines are far less inbred than the mouse lines used to examine the *Dlk1* mutation.

With this information in mind, it is potentially not surprising that morphological phenotypes that could be caused by *dlk2* mutation were not discovered in this study. There is a considerable difference in adipose development between the species, where adipose tissue is present at earlier mouse embryonic stages than zebrafish embryonic stages. In zebrafish, adipogenesis occurs outside of the developmental stages examined in this study, and size variation may be masked by genetic background effects.

6.3.2 Model of *dlk2* function in the embryonic neural progenitor cells

The *dlk2* mutation was bred into a Notch-responsive transgenic zebrafish in which a fluorescent protein is expressed where Notch signalling is active. Different embryonic time points were examined and co-localisation of the Notch signal with GFAP-positive cells (labelled by IHC) was examined. At 48 h.p.f., there was a large increase of GFAP positive cells not present in the wild type. BrdU staining confirmed that, at 48 h.p.f., these cells where highly proliferative, with the BrdU signal clearly co-localising to the GFAP positive cells. By 72 h.p.f., the pool of GFAP-positive cells was depleted relative to the wild type embryo. By the early larval stage there were almost no GFAP-positive cells in the mutant larvae, while there is a large number present in the wild type larvae. The exact nature of the GFAP-positive cells at this embryonic stage is not perfectly defined, but they are generally referred to as neural progenitors, radial glial cells or oligodendrocyte precursor cells (Appel et al., 2001; Zaucker et al., 2013). It is likely that they are a transit amplifying population, derived from NSCs derived from the developing neural epithelium. Early defects in neurogenesis have been identified previously in Notch mutants, such as *mind bomb*, which encodes E3 ubiquitin ligase required for effective Delta function (Bingham et al., 2003). *Notch3* zebrafish mutants also have reduced numbers of GFAP expressing cells at 52 h.p.f., which is a very similar phenotype to the *dlk2* mutant described in this thesis (Zaucker et al., 2013). This same neurogenic defect in zebrafish larvae has been described in a dominant negative mutation of

deltaA (Appel et al., 1999). In addition, behavioural deficits have previously been reported in the Notch-signalling perturbed mutants due to the increase in primary motorneurons at the cost of later-specified secondary motorneuron populations (Appel et al., 2001; Bingham et al., 2003). The similarity in phenotypes between the Notch-signalling perturbed mutants and the *dlk2* mutant described strongly supports the hypothesis that *dlk2* operates through the Notch signalling pathway in this context. In the existing literature, the hypothesis for the role of *dlk2* in the Notch signalling pathway is as an inhibitor of Notch, because it lacks essential Notch ligand binding domains (Bray et al., 2008).

In summary, the current model is that the NSCs in the early zebrafish embryo are regulated through lateral inhibition of Notch signalling. Small asymmetries in Notch activation in the heterogeneous NSC population are reinforced by expression of Delta in differentiating cells (low Notch signalling cells), in order to maintain high levels of Notch in the neighbouring cells. This balance between Notch and Delta signalling is the mechanism that maintains the NSC pool and controls the correct timing of differentiation of the transit amplifying cell populations, such that they receive the correct signalling information from other pathways and are specified into their correct neuronal fate (Appel et al., 2001). The results presented here could be interpreted as *dlk2* behaving as a Notch-activating ligand in the zebrafish embryonic brain, explaining the same phenotype in *dlk2* mutants as in Delta and Notch mutants. However, another hypothesis is that *dlk2* is behaving as a dominant negative Delta or a Delta antagonist. In this hypothesis, *dlk2* is operating to establish heterogeneity in Notch-signalling in the NSC populations, which facilitates the lateral inhibition mechanisms of the NSC fate regulation. If, in the wild type scenario, Notch is not correctly down-regulated in cells fated to differentiate, it could lead to a lack of Delta up-regulation in the few cells meant to differentiate. Therefore, high Notch signalling in the neighbouring cells would not be maintained, which in turn leads to abnormally high numbers of cells prematurely differentiating and a depletion of the stem cell pool. The results described in this

project are not sufficient to determine which of these two models is correct. Future experiments will need to be performed in order to elucidate the mechanism of *dlk2* function (Section 6.5.3).

6.4 Consequences of lacking adult radial glial cells in the telencephalon

The radial glial cells in the periventricular zone of the adult zebrafish telencephalon are known to play an important role in the regeneration of the brain upon injury (Baumgart et al., 2012; Chapouton et al., 2010; Kroehne et al., 2011). This study demonstrated that *dlk2* mutant zebrafish lack this cell population in the adult telencephalon. Similarly, adult mammalian brains do not have NSCs capable of regenerating following brain injury. When a brain injury occurs in mammals, there is a major inflammatory response, which activates microglia and macrophages. This results in a wave of neural degeneration, negative regulation of neurogenesis, and the formation of a glial scar (Ekdahl et al., 2003; Fitch and Silver, 2008; Silver and Miller, 2004). In zebrafish, there is an initial inflammatory response but it very quickly subsides, allowing for an environment that is permissive to neurogenesis and regeneration (Kroehne et al., 2011).

The *dlk2* mutant zebrafish can be used as a model to understand the response to injury in the adult telencephalon when the radial glial cells are absent. It would aid in understanding the responsibility this cell population has in regeneration, and whether regeneration is possible without it. In addition, the *dlk2* mutant zebrafish models opens up the possibility of understanding whether there is a permissive neurogenic environment even without radial glial cells, or if the inflammatory response is overwhelming in the absence of the NSCs responsible for re-populating the injury site, leading to scar formation. Understanding this process would be informative in understanding how to generate such regeneration-permissive environments within mammalian brains. In order to address such questions, a targeted ablation model, using the GFAP promoter, has been created (Shimizu et al., 2015). However, this approach is not completely effective at removing the radial glial cells. In addition, the ablation of all cells expressing GFAP will, most likely, have secondary

effects beyond just losing this cell population, which may confound the analysis of the radial glial cells in the regeneration process.

6.5 Future work

6.5.1 *Dlk2* in mouse

During this thesis, both *dlk1* and *dlk2* in zebrafish have been compared to *Dlk1* expression in murine development. *Dlk1* has been extensively studied in murine development and different stem cell populations. On the other hand, there has been very little descriptive or experimental work performed on *Dlk2,* and no *in vivo* examination. The aim of this study was to produce a model to understand the basal mechanism of operation of these genes; therefore, the justification for focusing on zebrafish *dlk2* and its comparison to murine *Dlk1* is two-fold:

i) The structural similarity between murine *Dlk1* and *Dlk2* is very high, suggesting a shared mechanistic operation. This would be similar to the reasonable assumption that different canonical Delta genes would operate through the same Notch-based mechanisms (such as *dll1, dll2* and others.*)*.

ii) Evolutionary analysis suggests that *Dlk2* is the ancestral gene, from which *Dlk1* was derived. Its sequence is much more highly conserved than *Dlk1*. This leads to the second assumption, which is that zebrafish *dlk2* function, particularly if shared with murine *Dlk1* function*,* is representative of the basal mechanism of function for these genes.

However, understanding the role of murine *Dlk2* would be extremely useful to make a thorough comparison between the two organisms. There is on-going work in the lab to describe the embryonic expression of murine *Dlk2* and to produce a *Dlk2* mutant mouse using the CRISPR-Cas9 technique (pers. comm. Alex Ashcroft). Initial *Dlk2* ISH analysis of mouse embryos show broad expression in the brain. This is similar to *dlk1* and *dlk2* expression in zebrafish embryos,

supporting the hypothesis that zebrafish *dlk1* and *dlk2* represent the ancestral functions of this gene family.

6.5.1 Further investigation of the phenotype of *dlk2* mutants

i) In depth exploration of the consequences of *dlk2* loss for embryonic NSC

The first question that needs to be addressed is whether the expansion of the transit amplifying GFAP-positive cell population is due to the premature differentiation of the earlier NSCs derived from the neural epithelium. The Notch-responsive reporter is a good model for gross Notch signalling examination, but not the best system for examining the fine details of these cell populations. Antibodies for Her6 and Sox2 would be ideal for examining the initial NSC population. Antibodies for DeltaA and Neurog1 would identify the cells that are beginning to differentiate (Schmidt et al., 2013). Using these markers will give a more precise understanding of the effect that the loss of *dlk2* has on these NSC populations.

ii) Behavioural analysis of *dlk2* mutant zebrafish

Preliminary results from the tracking of larvae zebrafish have suggested that the early larval *dlk2* mutants have increased levels of movement under normal conditions. This could be examined further by investigating the response of the larvae to a vibration stimulus, which is known to evoke a startle response, and their ability to habituate to this stimulus. The hypothesis is that this behavioural phenotype is due to the increase in primary motorneurons, and that lack of secondary-born motorneurons may lead to later behavioural defects that can be further examined using markers for the different neuronal types. The markers that can be used are outlined in previous studies (Appel et al., 2001; Bingham et al., 2003). Of particular interest would be *isl1,* a marker for presumptive primary motor neurons, and the zn-8 antibody, which is a marker for secondary motor neurons (Appel et al., 2001).

iii) Further examination of the mechanism of *dlk2* function

This thesis has produced a model system in which to examine the mechanism of *dlk2* in zebrafish. However, it currently does not provide sufficient evidence to determine this mechanism. The results demonstrate that *dlk2* mutant zebrafish have aberrant specification of NSCs in the embryonic brain. This leads to premature differentiation of these cells and in the subsequent depletion of this cell population. This same phenotype is also observed in Delta and Notch mutants (Appel et al., 1999; Appel et al., 2001; Bingham et al., 2003; Zaucker et al., 2013). From the results obtained to date, it is not possible to determine whether *dlk2* is operating as a Notch-activating ligand or a Notch antagonist. In order to examine this, a targeted knock-down or knock-out in the NSC of *dlk2* could be performed. Notch signalling in adjacent cells should then be observed and ultimately these could be lineage traced to determine the role of *dlk2*. This could be performed by a conditional *dlk2* mutant, using a Cre recombinase approach (Ni et al., 2012). Alternatively, a photo-cleavable morpholino (MO) approach could be used. Combination of a photo-sensitive moiety into the MO structure allows the MO to be either activated or inactivated by UV photolysis (Sumanas, 2017; Tallafuss et al., 2012). Since the results presented in Section 2.3 show that *dlk2* MO injected zebrafish do have a reduction in DLK2 protein, further studies could be performed using photo-activatable forms of the *dlk2* MO. This would allow both temporal and spatial knock-down of *dlk2* in targeted NSC(s), followed by the examination of the Notch signalling in adjacent cells and would eliminate the confounding effects of knockdown on earlier developmental events.

iv) The role of *dlk2* in zebrafish adipogenesis

Murine *Dlk1* has been shown to inhibit the differentiation of pre-adipocytes into mature adipocytes (Sul, 2009). In addition, an obesity phenotype is described in the *Dlk1* mutant mouse (Moon et al., 2002). Zebrafish has been studied as a model for adipogenesis and obesity (Flynn et al., 2009; Oka et al., 2010). It would be interesting to examine the histology and development of the adipose tissue in the *dlk2* mutant to examine if it has a role in adipogenesis, similar to the role of murine *Dlk1* and also that hypothesised for murine *Dlk2* (Nueda et al., 2007).

6.5.4 *Dlk1* in zebrafish

During this thesis, an attempt was made to modulate *dlk1* in zebrafish using MOs and to produce a *dlk1* mutant using the CRISPR-Cas9 technology. Unfortunately, neither of these attempts were successful and a zebrafish *dlk1* model has not been established. It would be hugely beneficial to the understanding of *dlk1* to produce a zebrafish mutant at this gene locus. An attempt has been made to produce a null mutation of *Dlk2* in mouse using CRISPR-Cas9 and it is proving equally difficult, even though other genes were targeted at the same time and have been successful (Data not published, pers. comm. Anne Ferguson-Smith). This suggests that these genes may be particularly hard to mutate using the CRISPR-Cas9 system. However, TALENs have been successfully employed for targeted mutation in zebrafish and these could be used to attempt to mutate the *dlk1* gene locus (Zu et al., 2013).

6.5.5 Examination of the role of radial glial cells using a model that has no radial glial cells.

The radial glial cells in the periventricular zone of the adult zebrafish telencephalon have been shown to be responsible for the regeneration of the telencephalon upon injury (Kroehne et al.,

2011). What would occur in a system where there is no radial glial cell present when the injury occurs is currently not known. The established brain stab model could be employed to assess this (Baumgart et al., 2012). In this model, the adult zebrafish are stabbed with a needle through a nostril into one lobe of the telencephalon. The lesion created is then examined in a time series from the time of injury. Of particular interest, this experiment would examine whether regeneration is still possible and whether other cells would fill the role of radial glial cells. Furthermore, the experiment could show whether the inflammation response, which leads to glial scars in mammals, would be as limited as usual or if the presence of the radial glial cells is essential for promoting a regenerative environment (Baumgart et al., 2012).

In summary, the present study has shown that zebrafish are a valuable model to investigate the ancestral functions of *dlk1* and *dlk2*. The discovery that *dlk2* loss of function results in an absence of adult radial glia cells reveals an important role for this protein in the regulation of zebrafish NSCs. This study has identified a novel model that could be used to explore the role of radial glial cells in regeneration and may lead to important discoveries as to the role and mechanistic functions of the *Dlk1* and *Dlk2* genes.

Bibliography

Appel, B., Fritz, A., Westerfield, M., Grunwald, D. J., Eisen, J. S. and Riley, B. B. (1999). Delta-mediated specification of midline cell fates in zebrafish embryos. *Current Biology* 9, 247–257.

Appel, B., Givan, L. A. and Eisen, J. S. (2001). Delta-Notch signaling and lateral inhibition in zebrafish spinal cord development. *BMC Dev. Biol.* 1, 13.

Bachmann, E., Krogh, T. N., Højrup, P., Skjødt, K. and Teisner, B. (1996). Mouse fetal antigen 1 (mFA1), the circulating gene product of mdlk, pref-1 and SCP-1: isolation, characterization and biology. *J Reprod Fertil* 107, 279–285.

Baisong Mei, L. Z. L. C. H. S. S. (2002). Only the large soluble form of preadipocyte factor-1 (Pref-1), but not the small soluble and membrane forms, inhibits adipocyte differentiation: role of alternative splicing. *Biochemical Journal* 364, 137.

Baladrón, V., Ruiz-Hidalgo, M.-J., Nueda, M.-L., Díaz-Guerra, M.-J. M., García-Ramírez, J.-J., Bonvini, E., Gubina, E. and Laborda, J. (2005). dlk acts as a negative regulator of Notch1 activation through interactions with specific EGF-like repeats. *Exp. Cell Res.* 303, 343–359.

Baumgart, E. V., Barbosa, J. S., Bally-Cuif, L., Götz, M. and Ninkovic, J. (2012). Stab wound injury of the zebrafish telencephalon: A model for comparative analysis of reactive gliosis. *Glia* 60, 343–357.

Bingham, S., Chaudhari, S., Vanderlaan, G., Itoh, M., Chitnis, A. and Chandrasekhar, A. (2003). Neurogenic phenotype of mind bomb mutants leads to severe patterning defects in the zebrafish hindbrain. *Dev. Dyn.* 228, 451–463.

Bray, S. J., Takada, S., Harrison, E., Shen, S.-C. and Ferguson-Smith, A. C. (2008). The atypical mammalian ligand Delta-like homologue 1 (Dlk1) can regulate Notch signalling in Drosophila. *BMC Dev. Biol.* 8, 11.

Burger, A., Lindsay, H., Felker, A., Hess, C., Anders, C., Chiavacci, E., Zaugg, J., Weber, L. M., Catena, R., Jinek, M., et al. (2016). Maximizing mutagenesis with solubilized CRISPR-Cas9 ribonucleoprotein complexes. *Development* 143, 2025–2037.

CANNON, B. and Nedergaard, J. (2004). Brown Adipose Tissue: Function and Physiological Significance. *Physiological Reviews* 84, 277–359.

Chapouton, P., Skupien, P., Hesl, B., Coolen, M., Moore, J. C., Madelaine, R., Kremmer, E., Faus-Kessler, T., Blader, P., Lawson, N. D., et al. (2010). Notch activity levels control the balance between quiescence and recruitment of adult neural stem cells. *Journal of Neuroscience* 30, 7961–7974.

Chapouton, P., Webb, K. J., Stigloher, C., Alunni, A., Adolf, B., Hesl, B., Topp, S., Kremmer, E. and Bally-Cuif, L. (2011). Expression of Hairy/enhancer of split genes in neural progenitors and neurogenesis domains of the adult zebrafish brain. *J. Comp. Neurol.* 519, 1748–1769.

Charalambous, M., da Rocha, S. T. and Ferguson-Smith, A. C. (2007). Genomic imprinting, growth control and the allocation of nutritional resources: consequences for postnatal life. *Current Opinion in Endocrinology, Diabetes and Obesity* 14, 3–12.

Charalambous, M., Ferron, S. R., da Rocha, S. T., Murray, A. J., Rowland, T., Ito, M., Schuster-Gossler, K., Hernandez, A. and Ferguson-Smith, A. C. (2012). Imprinted gene dosage is critical for the transition to independent life. *Cell Metab.* 15, 209–221.

Cleaton, M. A. M., Dent, C. L., Howard, M., Corish, J. A., Gutteridge, I., Sovio, U., Gaccioli, F., Takahashi, N., Bauer, S. R., Charnock-Jones, D. S., et al. (2016). Fetus-derived DLK1 is required for maternal metabolic adaptations to pregnancy and is associated with fetal growth restriction. *Nature genetics* 48, 1473–1480.

Cordle, J., Johnson, S., Zi Yan Tay, J., Roversi, P., Wilkin, M. B., de Madrid, B. H., Shimizu, H., Jensen, S., Whiteman, P., Jin, B., et al. (2008). A conserved face of the Jagged/Serrate DSL domain is involved in Notch trans-activation and cis-inhibition. *Nat. Struct. Mol. Biol.* 15, 849–857.

da Rocha, S. T. S., Tevendale, M. M., Knowles, E. E., Takada, S. S., Watkins, M. M. and Ferguson-Smith, A. C. A. (2007). Restricted co-expression of Dlk1 and the reciprocally imprinted non-coding RNA, Gtl2: implications for cis-acting control. *Developmental Biology* 306, 810–823.

da Rocha, S. T. D., Edwards, C. A., Ito, M., Ogata, T., & Ferguson-Smith, A. C. (2008). Genomic imprinting at the mammalian Dlk1-Dio3 domain. *Trends in Genetics*, *24*(6), 306–316. http://doi.org/10.1016/j.tig.2008.03.011

da Rocha, S. T., Charalambous, M., Lin, S.-P., Gutteridge, I., Ito, Y., Gray, D., Dean, W. and Ferguson-Smith, A. C. (2009). Gene dosage effects of the imprinted delta-like homologue 1 (dlk1/pref1) in development: implications for the evolution of imprinting. *PLoS genetics* 5, e1000392–e1000392.

Dieterlen-Lievre, F. (1975). On the origin of haemopoietic stem cells in the avian embryo: an experimental approach. *J Embryol Exp Morphol* 33, 607–619.

Edwards, C. A., Mungall, A. J., Matthews, L., Ryder, E., Gray, D. J., Pask, A. J., Shaw, G., Graves, J. A. M., Rogers, J., SAVOIR consortium, et al. (2008). The evolution of the DLK1-DIO3 imprinted domain in mammals. *PLoS Biology* 6, e135.

Eisen, J. S. and Smith, J. C. (2008). Controlling morpholino experiments: don't stop making antisense. *Development* 135, 1735–1743.

Ekdahl, C. T., Claasen, J.-H., Bonde, S., Kokaia, Z. and Lindvall, O. (2003). Inflammation is detrimental for neurogenesis in adult brain. *Proceedings of the National Academy of Sciences* 100, 13632–13637.

Ferrón, S. R., Charalambous, M., Radford, E., McEwen, K., Wildner, H., Hind, E., Morante-Redolat, J. M., Laborda, J., Guillemot, F., Bauer, S. R., et al. (2011). Postnatal loss of Dlk1 imprinting in stem cells and niche astrocytes regulates neurogenesis. *Nature* 475, 381–385.

Fitch, M. T. and Silver, J. (2008). CNS injury, glial scars, and inflammation: Inhibitory extracellular matrices and regeneration failure. *Exp. Neurol.* 209, 294–301.

Flynn, E. J., Trent, C. M. and Rawls, J. F. (2009). Ontogeny and nutritional control of adipogenesis in zebrafish (Danio rerio). *The Journal of Lipid Research* 50, 1641–1652.

Herrera, E. and Amusquivar, E. (2000). Lipid metabolism in the fetus and the newborn.

Diabetes/Metabolism Research and Reviews 16, 202–210.

Johnson, K., Barragan, J., Bashiruddin, S., Smith, C. J., Tyrrell, C., Parsons, M. J., Doris, R., Kucenas, S., Downes, G. B., Velez, C. M., et al. (2016). Gfap-positive radial glial cells are an essential progenitor population for later-born neurons and glia in the zebrafish spinal cord. *Glia* 64, 1170–1189.

Kim, K.-A., Kim, J.-H., Wang, Y. and Sul, H. S. (2007). Pref-1 (preadipocyte factor 1) activates the MEK/extracellular signal-regulated kinase pathway to inhibit adipocyte differentiation. *Mol Cell Biol* 27, 2294–2308.

Kimmel, C. B., Ballard, W. W., Kimmel, S. R., Ullmann, B. and Schilling, T. F. (1995). Stages of embryonic development of the zebrafish. *Dev. Dyn.* 203, 253–310.

Kok, F. O., Shin, M., Ni, C.-W., Gupta, A., Grosse, A. S., van Impel, A., Kirchmaier, B. C., Peterson-Maduro, J., Kourkoulis, G., Male, I., et al. (2015). Reverse Genetic Screening Reveals Poor Correlation between Morpholino-Induced and Mutant Phenotypes in Zebrafish. *Developmental cell* 32, 97–108.

Kopan, R. and Ilagan, M. (2009). The Canonical Notch Signaling Pathway: Unfolding the Activation Mechanism. *Cell*.

Kroehne, V., Freudenreich, D., Hans, S., Kaslin, J. and Brand, M. (2011). Regeneration of the adult zebrafish brain from neurogenic radial glia-type progenitors. *Development* 138, 4831–4841.

Laborda, J., Sausville, E. A., Hoffman, T. and Notario, V. (1993). dlk, a putative mammalian homeotic gene differentially expressed in small cell lung carcinoma and neuroendocrine tumor cell line. *J. Biol. Chem.* 268, 3817–3820.

Le Cong, Ran, F. A., Cox, D., Lin, S., Barretto, R., Habib, N., Hsu, P. D., Wu, X., Jiang, W., Marraffini, L. A., et al. (2013). Multiplex Genome Engineering Using CRISPR/Cas Systems. *Science* 339, 819–823.

Ma, D. K., Bonaguidi, M. A., Ming, G.-L. and Song, H. (2009). Adult neural stem cells in the mammalian central nervous system. *Cell Res* 19, 672–682.

Mabee, P. M., Olmstead, K. L. and Cubbage, C. C. (2009). AN EXPERIMENTAL STUDY OF INTRASPECIFIC VARIATION, DEVELOPMENTAL TIMING, AND HETEROCHRONY IN FISHES. *http://dx.doi.org/10.1554/0014-3820(2000)054[2091:AESOIV]2.0.CO;2* 54, 2091.

März, M., Chapouton, P., Diotel, N., Vaillant, C., Hesl, B., Takamiya, M., Lam, C. S., Kah, O., Bally-Cuif, L. and Strähle, U. (2010). Heterogeneity in progenitor cell subtypes in the ventricular zone of the zebrafish adult telencephalon. *Glia* 58, 870–888.

Mirshekar-Syahkal, B., Haak, E., Kimber, G. M., van Leusden, K., Harvey, K., O'Rourke, J., Laborda, J., Bauer, S. R., de Bruijn, M. F. T. R., Ferguson-Smith, A. C., et al. (2013). Dlk1 is a negative regulator of emerging hematopoietic stem and progenitor cells. *Haematologica* 98, 163–171.

Moon, Y. S., Smas, C. M., Lee, K., Villena, J. A., Kim, K.-H., Yun, E. J. and Sul, H. S. (2002).

Mice Lacking Paternally Expressed Pref-1/Dlk1 Display Growth Retardation and Accelerated Adiposity. *Mol Cell Biol* 22, 5585–5592.

Ni, T. T., Lu, J., Zhu, M., Maddison, L. A., Boyd, K. L., Huskey, L., Ju, B., Hesselson, D., Zhong, T. P., Page-McCaw, P. S., et al. (2012). Conditional control of gene function by an invertible gene trap in zebrafish. *P Natl Acad Sci Usa* 109, 15389–15394.

Nueda, M.-L., Baladrón, V., García-Ramírez, J.-J., Sánchez-Solana, B., Ruvira, M.-D., Rivero, S., Ballesteros, M.-Á., Monsalve, E.-M., Díaz-Guerra, M.-J. M., Ruiz-Hidalgo, M.-J., et al. (2007). The Novel Gene EGFL9/Dlk2, Highly Homologous to Dlk1, Functions as a Modulator of Adipogenesis. *J Mol Biol* 367, 1270–1280.

Oka, T., Nishimura, Y., Zang, L., Hirano, M., Shimada, Y., Wang, Z., Umemoto, N., Kuroyanagi, J., Nishimura, N. and Tanaka, T. (2010). Diet-induced obesity in zebrafish shares common pathophysiological pathways with mammalian obesity. *BMC Physiology 2010 10:1* 10, 21.

Parant, J. M., George, S. A., Pryor, R., Wittwer, C. T. and Yost, H. J. (2009). A rapid and efficient method of genotyping zebrafish mutants. *Dev. Dyn.* 238, 3168–3174.

Paridaen, J. T. and Huttner, W. B. (2014). Neurogenesis during development of the vertebrate central nervous system. *EMBO reports* 15, 351–364.

Parsons, M. J., Pisharath, H., Yusuff, S., Moore, J. C., Siekmann, A. F., Lawson, N. and Leach, S. D. (2009). Notch-responsive cells initiate the secondary transition in larval zebrafish pancreas. *Mechanisms of Development* 126, 898–912.

PARTRIDGE, M., VINCENT, A., MATTHEWS, P., PUMA, J., STEIN, D. and SUMMERTON, J. (2009). A Simple Method for Delivering Morpholino Antisense Oligos into the Cytoplasm of Cells. *http://www.liebertpub.com/oli* 6, 169–175.

Reynolds, B. A. and Rietze, R. L. (2005). Neural stem cells and neurospheres—re-evaluating the relationship. *Nat. Methods* 2, 333–336.

Rossi, A., Kontarakis, Z., Gerri, C., Nolte, H., Hölper, S., Krüger, M. and Stainier, D. Y. R. (2015). Genetic compensation induced by deleterious mutations but not gene knockdowns. *Nature* 524, 230–233.

Rugh, R. (1968). CAB Direct. *The mouse Its reproduction and development*.

Schmidt, R., Strähle, U. and Scholpp, S. (2013). Neurogenesis in zebrafish – from embryo to adult. *Neural Dev* 8, 3.

Shimizu, Y., Ito, Y., Tanaka, H. and Ohshima, T. (2015). Radial glial cell-specific ablation in the adult Zebrafish brain. *genesis* 53, 431–439.

Silver, J. and Miller, J. H. (2004). Regeneration beyond the glial scar. *Nature reviews. Neuroscience* 5, 146–156.

Smas, C. M. and Sul, H. S. (1993). Pref-1, a protein containing EGF-like repeats, inhibits adipocyte differentiation. *Cell* 73, 725–734.

Sul, H. S. (2009). Minireview: Pref-1: role in adipogenesis and mesenchymal cell fate. *Mol.*

Endocrinol. 23, 1717–1725.

Sumanas, S. (2017). Inducible Inhibition of Gene Function with Photomorpholinos. In *Morpholino Oligomers* (eds. Moulton, H. M. and Moulton, J. D., pp. 51–57. New York, NY: Springer New York.

SUMMERTON, J. and WELLER, D. (1997). Morpholino Antisense Oligomers: Design, Preparation, and Properties. *Antisense and Nucleic Acid Drug Development* 7, 187–195.

Sun, X. and Artavanis-Tsakonas, S. (1996). The intracellular deletions of Delta and Serrate define dominant negative forms of the Drosophila Notch ligands. *Development* 122, 2465–2474.

Surmacz, B., Noisa, P., Risner-Janiczek, J. R., Hui, K., Ungless, M., Cui, W. and Li, M. (2011). DLK1 Promotes Neurogenesis of Human and Mouse Pluripotent Stem Cell-Derived Neural Progenitors Via Modulating Notch and BMP Signalling. *Stem Cell Rev and Rep* 8, 459–471.

Tallafuss, A., Gibson, D., Morcos, P., Li, Y., Seredick, S., Eisen, J. and Washbourne, P. (2012). Turning gene function ON and OFF using sense and antisense photo-morpholinos in zebrafish. *Development* 139, 1691–1699.

Wang, Y., Kim, K.-A., Kim, J.-H. and Sul, H. S. (2006). Pref-1, a preadipocyte secreted factor that inhibits adipogenesis. *J. Nutr.* 136, 2953–2956.

Westerfield, M., Zon, L. I. and Detrich, H. W., III (2009). Essential Zebrafish Methods.

Wu, X., Scott, D. A., Kriz, A. J., Chiu, A. C., Hsu, P. D., Dadon, D. B., Cheng, A. W., Trevino, A. E., Konermann, S., Chen, S., et al. (2014). Genome-wide binding of the CRISPR endonuclease Cas9 in mammalian cells. *Nat. Biotechnol.* 32, 670–676.

Yevtodiyenko, A. and Schmidt, J. V. (2006). Dlk1 expression marks developing endothelium and sites of branching morphogenesis in the mouse embryo and placenta. *Dev. Dyn.* 235, 1115–1123.

Zaucker, A., Mercurio, S., Sternheim, N., Talbot, W. S. and Marlow, F. L. (2013). notch3 is essential for oligodendrocyte development and vascular integrity in zebrafish. *Disease Models & Mechanisms* 6, 1246–1259.

Zhang, J. and Jiao, J. (2015). Molecular Biomarkers for Embryonic and Adult Neural Stem Cell and Neurogenesis. *BioMed Research International* 2015, 1–14.

Zu, Y., Tong, X., Wang, Z., Liu, D., Pan, R., Li, Z., Hu, Y., Luo, Z., Huang, P., Wu, Q., et al. (2013). TALEN-mediated precise genome modification by homologous recombination in zebrafish. *Nat. Methods* 10, 329–331.